

# Space weather impact on radio wave propagation

Norbert Jakowski

German Aerospace Center (DLR), Institute for Solar-Terrestrial Physics, Neustrelitz, Germany



Knowledge for Tomorrow



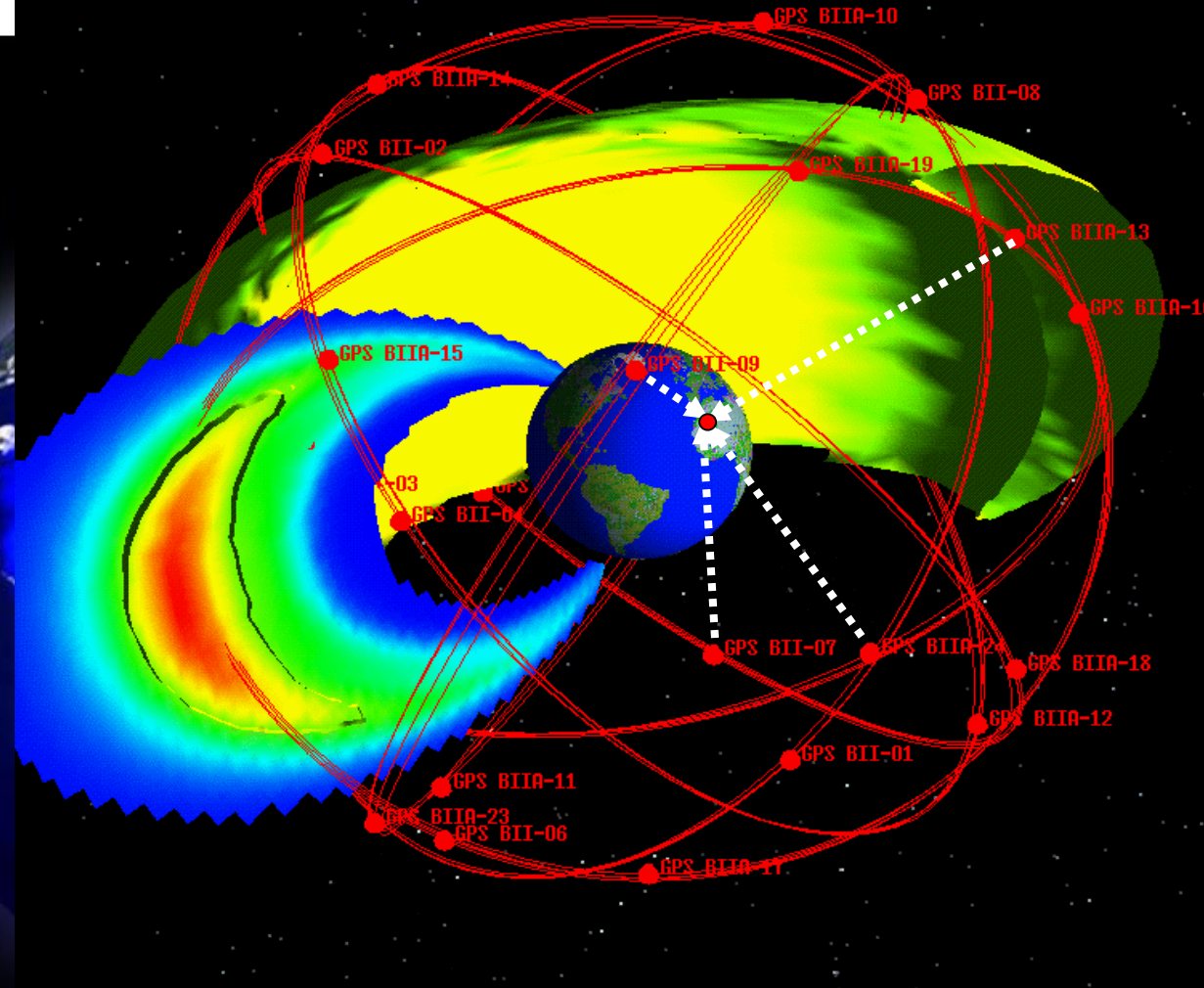
# Outline

- Introduction
  - Space weather
  - Ionosphere
- Radio wave propagation and ionosphere
  - The ionosphere
  - Fundamentals of radio wave propagation
- Ionospheric impact on radio systems
  - Telecommunication
  - Space based navigation
  - Remote sensing
- Summary



# Space Weather

## GNSS satellite orbits embedded in the geo-plasma



Radio waves play a significant role in modern technological systems:

- Terrestrial and space based telecommunication
- Ground and space based navigation systems (e.g. GNSS)
- Remote sensing radars

Space weather refers to the conditions on the Sun and in the solar wind, magnetosphere, ionosphere and thermosphere that can influence the performance and reliability of space-borne and ground-based technological systems and can endanger human life or health.

Definition NSWP, USA, 1996

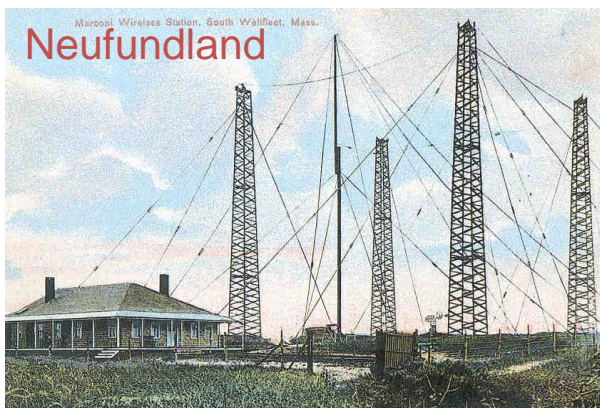
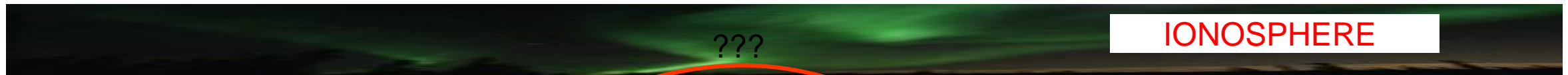
Credit: NASA





# History of electromagnetism - radio waves

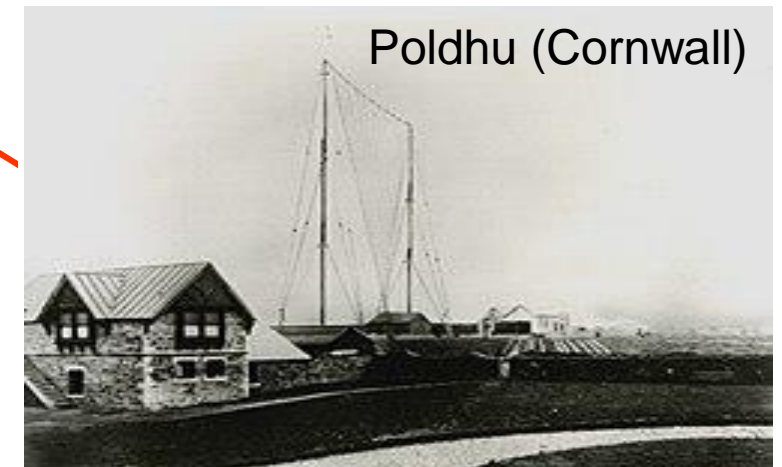
- James Clark Maxwell (1862) Theory of electromagnetism
- Heinrich Rudolf Hertz(1886) Approval of the existence of electromagnetic waves
- Guglielmo Marconi (1901) Transatlantic radio transmission (Nobel prize 1909)
- Oliver Heaviside and Ernest Kennelly (1902) Assumption of an electrically conductive layer in the atmosphere
- Edward. V. Appleton (1927- 32) **Theory of radio wave propagation in plasma** (Nobel prize 1947)



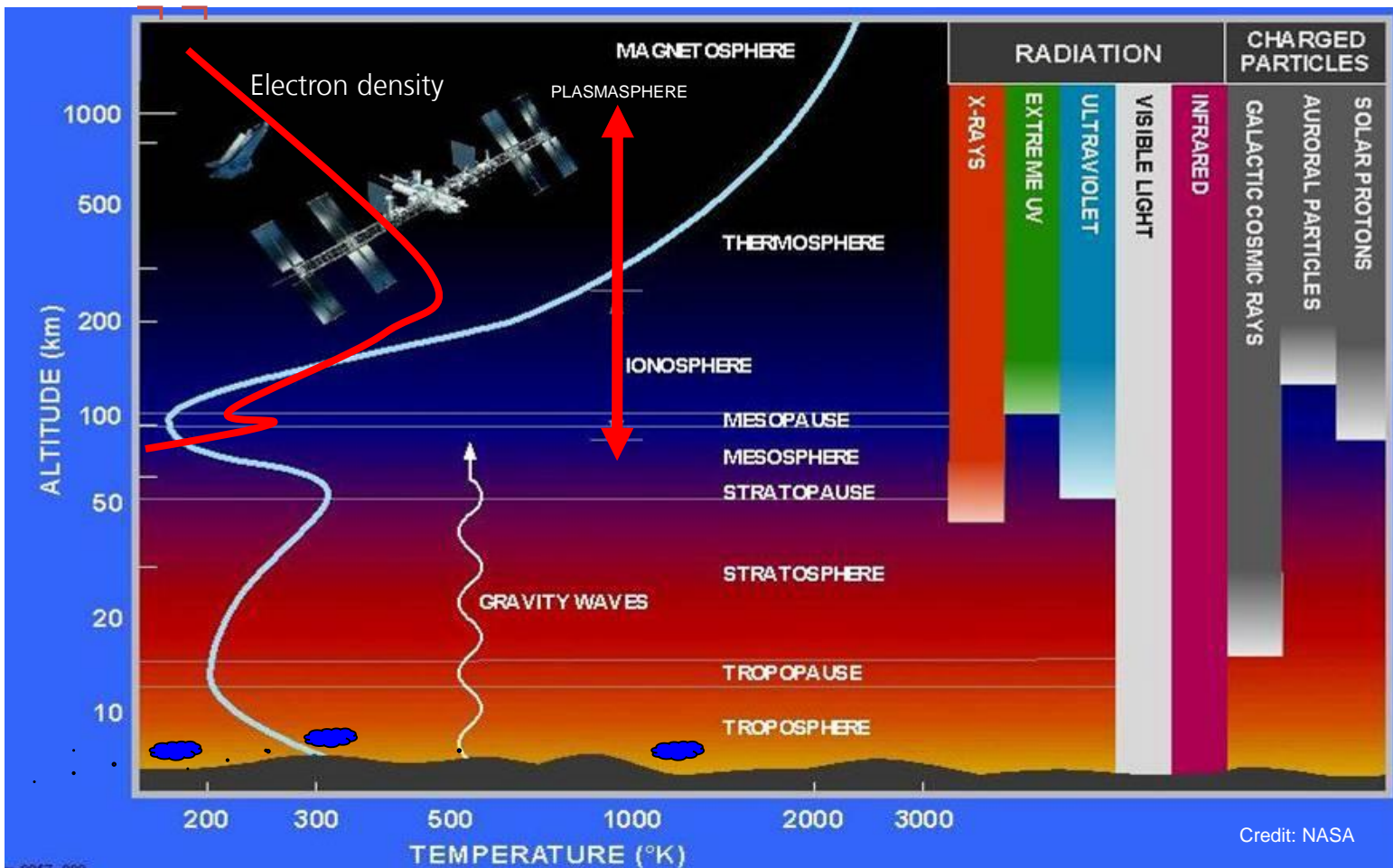
3500 km

Marconi's successful experiment demonstrates the close relationship between radio wave propagation and ionosphere - up today.

Ionosphere is a component of space weather.



# The Ionosphere/plasmasphere - integral part of the Geo-sphere



The Ionosphere/plasmasphere is an integral part of the Earth's environment and is characterized by strong coupling with other geo-spheres.

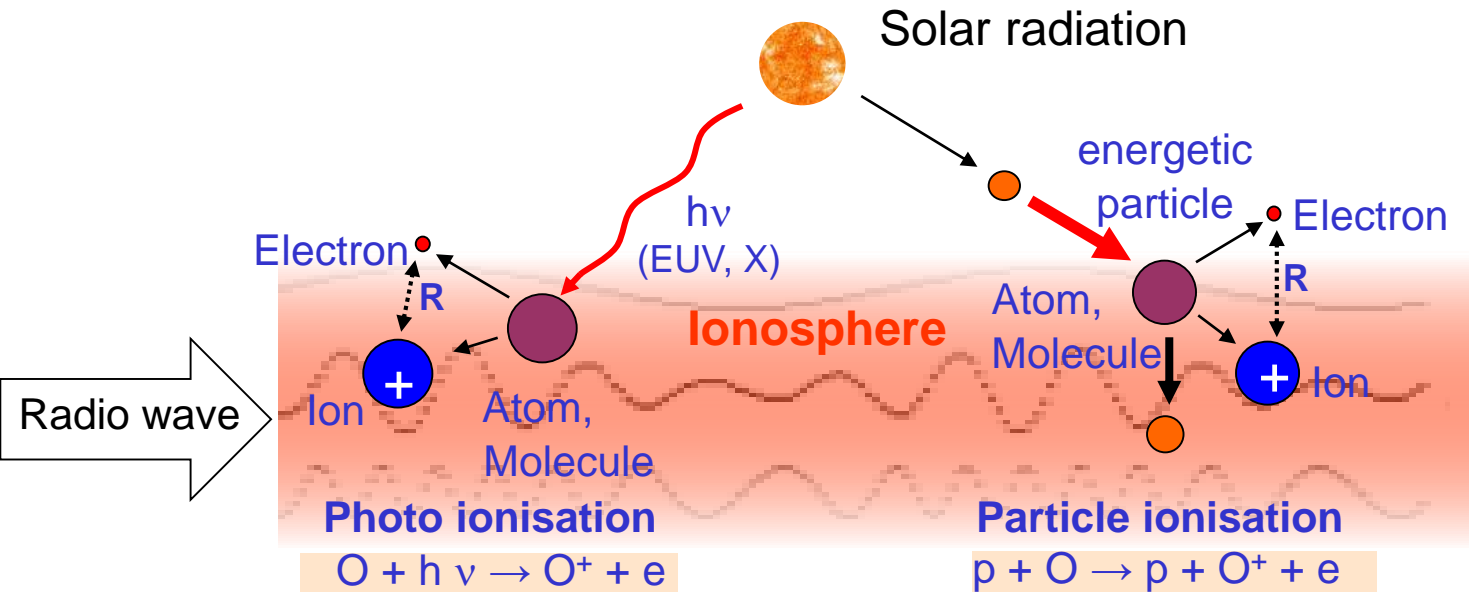
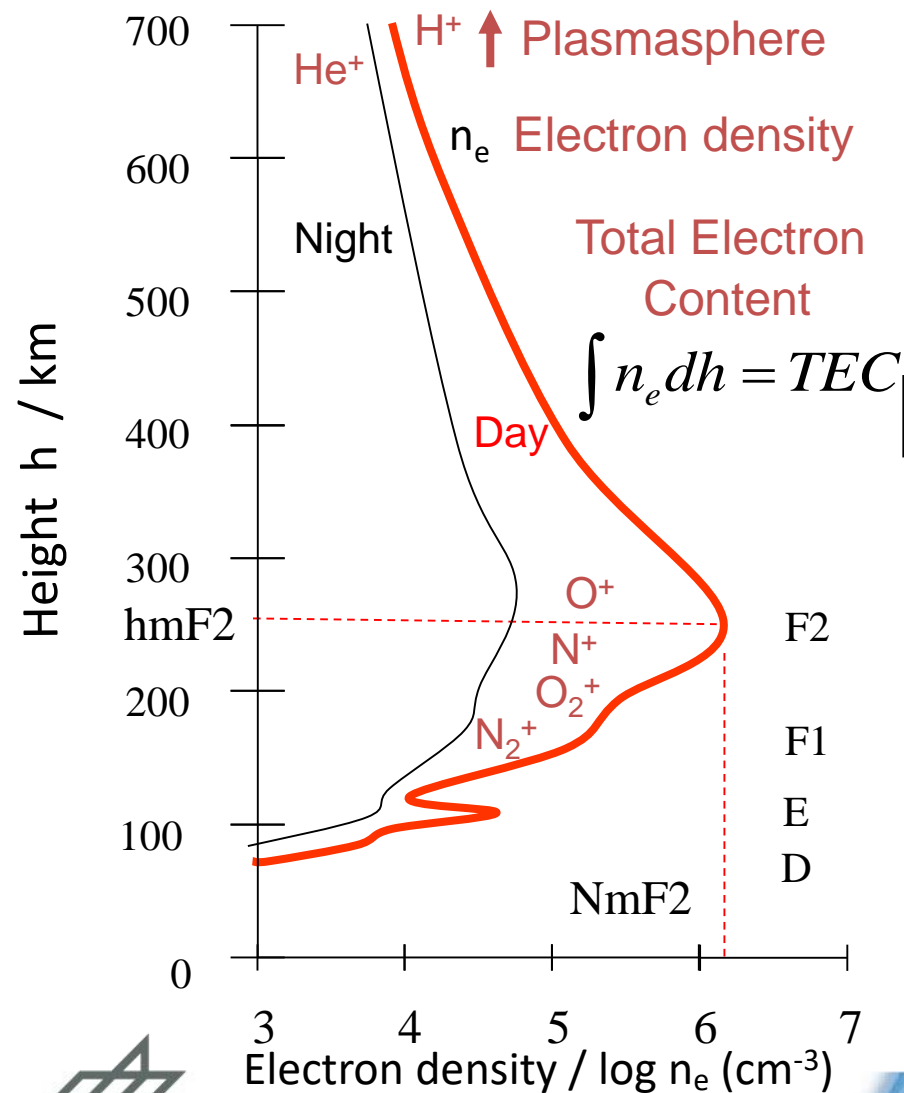
All geo-spheres are strongly impacted by the electromagnetic and corpuscular radiation of the sun.

The ionospheric plasma is mainly formed by solar radiation at wavelengths  $< 130$  nm.

Solar storms and associated Coronal Mass Ejections (CMEs) may heavily disturb the ionospheric and plasmaspheric behaviour.



# The ionosphere - ionized part of the atmosphere



## Ionosphere as the ionized part of the Earth's atmosphere

- is generated by electromagnetic and particle radiation from the sun
- is closely coupled with other geospheres such as the upper atmosphere, thermosphere and magnetosphere
- impacts propagation of electromagnetic radio waves,
- measurable changes of wave parameters **amplitude, phase, polarization** due to **absorption, refraction, diffraction, scattering**



# Refractive index of the ionospheric plasma

electromagnetic plane wave based on Maxwell's theory:

$$\vec{E} = A(\vec{k}) \cdot \exp\left(i(\omega(\vec{k}) \cdot t - \vec{k} \cdot \vec{r})\right)$$

$$v_{\varphi} = \frac{2\pi \cdot f}{k} \text{ phase velocity} \quad \vec{k} \text{ wave vector} \quad k = \frac{\omega}{c} = \frac{2 \cdot \pi}{\lambda}$$

Refractive index for a magnetized plasma (Appleton equation)

$$n^2 = 1 - \frac{X}{1 - iZ - \frac{Y^2 \sin^2 \Theta}{2(1 - X - iZ)} \pm Y \left[ \frac{Y^2 \sin^4 \Theta}{4(1 - X - iZ)^2} + \cos^2 \Theta \right]^{1/2}}$$

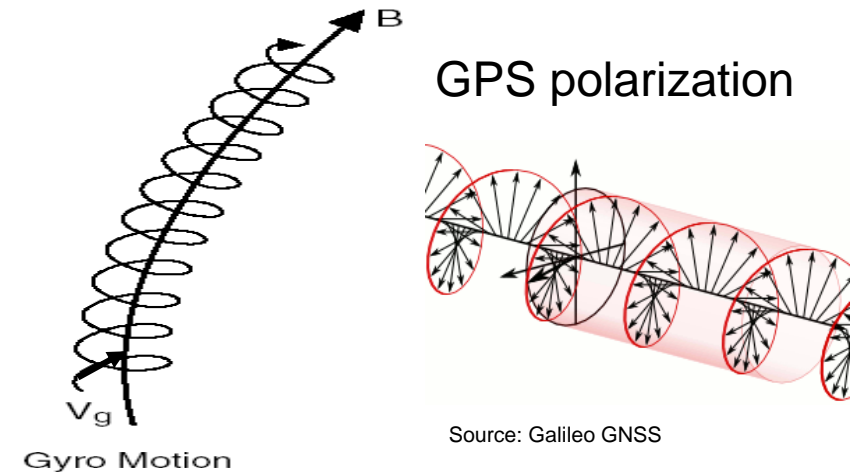
double refraction

$$X = \frac{f_p^2}{f^2}$$

$$Y = \frac{f_g}{f}$$

$$Z = \frac{\nu}{2\pi \cdot f}$$

$f_p$  : plasma frequency     $f_g$  : gyro frequency     $\nu$ : collision frequency



Gyro motion of electrons  
Electrons gyrate around  
geomagnetic field lines

$\Theta$  angle between ray path and geomagnetic field

Absorption can be ignored at GNSS frequencies.  
Refractive index depends on electron density and  
magnetic field vector.

Ionosphere is anisotropic due to the presence of  
the geomagnetic field.



# Refractive index of ionospheric plasma ( $f \gg f_p$ )

$$n \approx 1$$

$$- \frac{f_p^2}{2f^2}$$

First – order  
< 100 m L1

$$\pm \frac{f_p^2 f_g \cos \Theta}{2f^3}$$

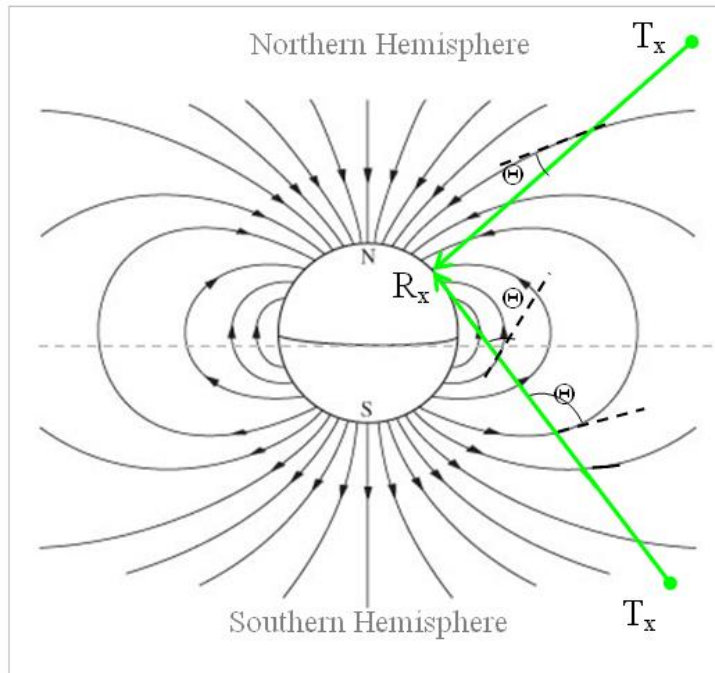
Second – order  
< 20 cm L1

$$- \frac{f_p^4}{8f^4}$$

Third – order  
< 1 cm L1

term

$$v_{phase} = \frac{c}{n}$$



Plasma frequency:

$$f_p = \sqrt{e^2 n_e / (4\pi^2 m_e \epsilon_0)} < \approx 20 \text{ MHz}$$

Gyro frequency:

$$f_g = eB / 2\pi \cdot m_e < \approx 1.5 \text{ MHz}$$

$\Theta$ : angle between wave direction and field vector  $\mathbf{B}$ ;

$n_e$ : electron density

$m_e$ : electron mass;  $B$ : magnetic induction

$\epsilon_0$ : free space permittivity

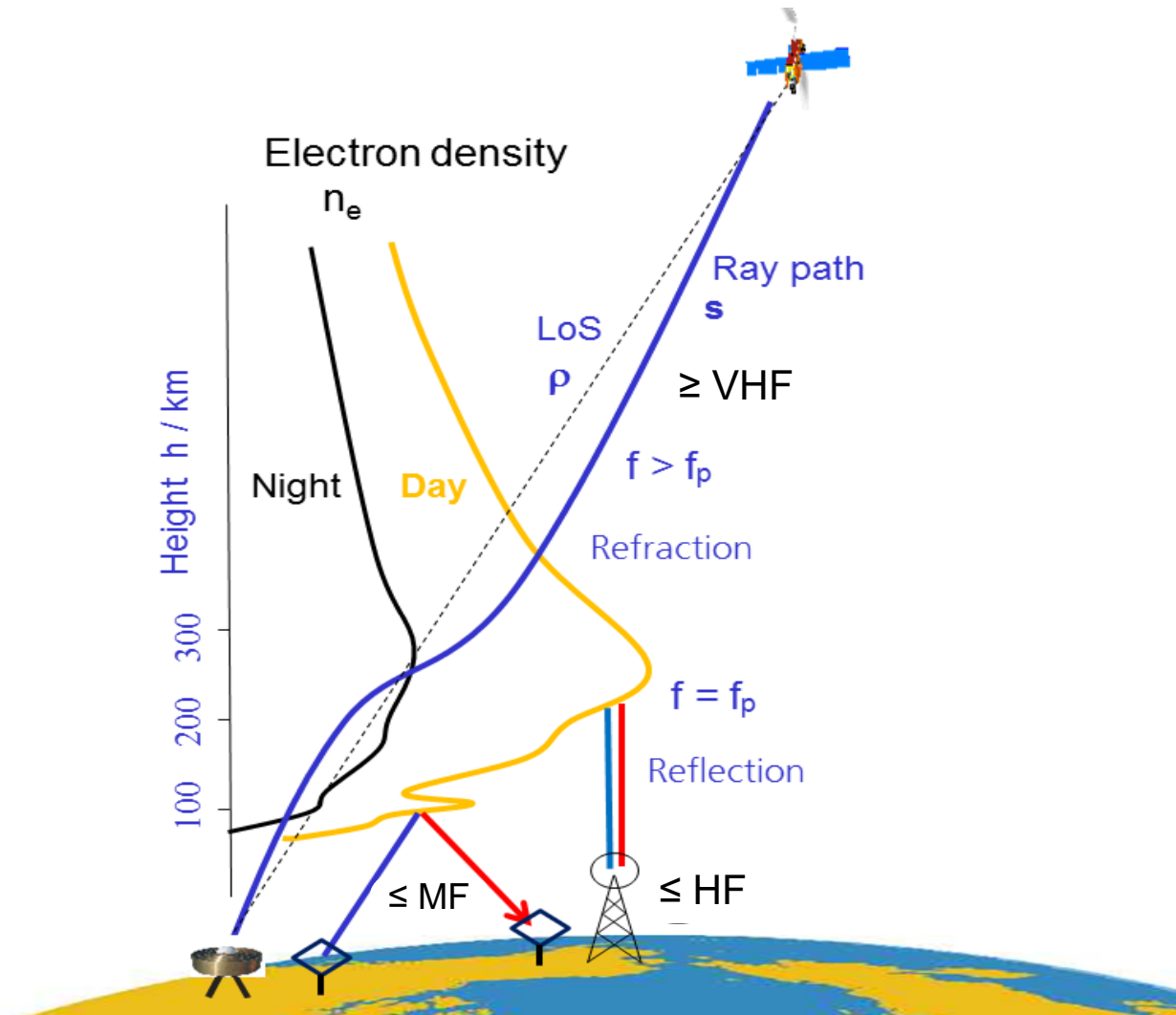
$f$ : signal frequency

Hoque, M.M., and N. Jakowski (2006). Higher order Effects in Precise Positioning,  
J. of Geodesy, 10.1007/s00190-006-0106-0





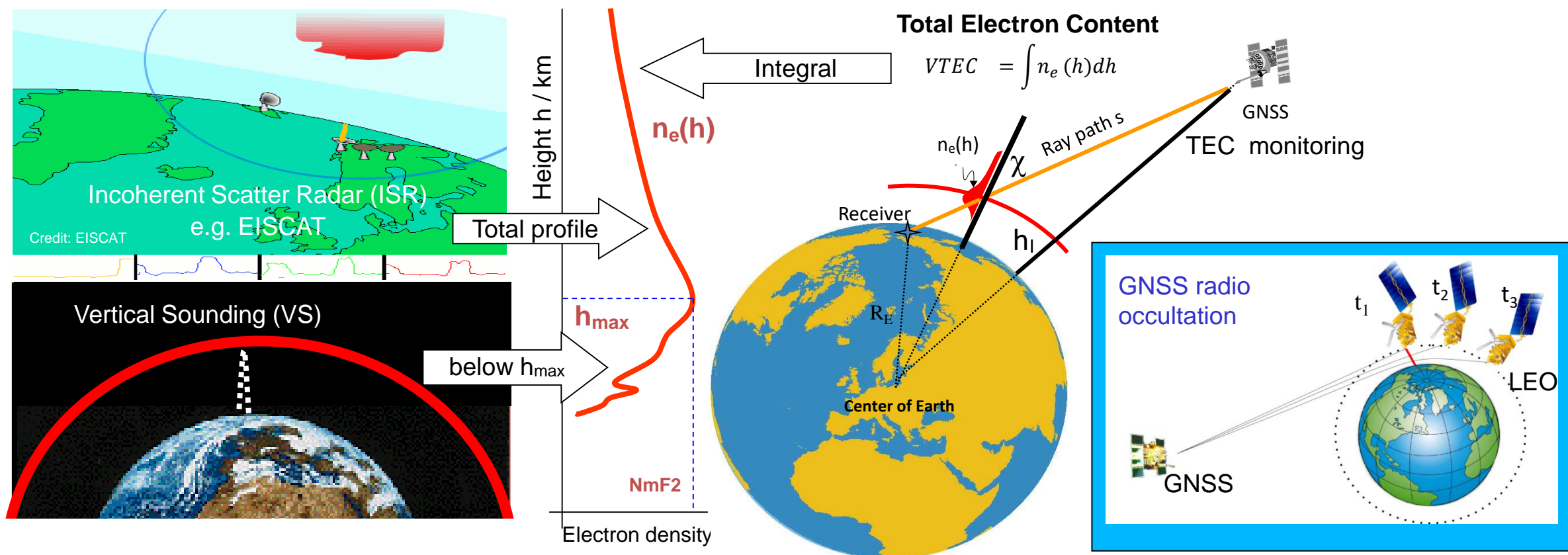
# Radio frequency spectrum & propagation



Symbol of frequency band	Frequency range	Wavelength range
ELF Extreme Low Frequency	< 300 Hz	> 1000 km
ULF Ultra Low Frequency	300 Hz - 3 kHz	1000 - 100 km
VLF Very Low Frequency	3 kHz - 30 kHz	100 - 10 km
LF Low Frequency	30 kHz - 300 kHz	10 - 1 km
MF Medium Frequency	300 kHz - 3 MHz	1000 - 100 m
HF High Frequency	3 MHz - 30 MHz	100 - 10 m
VHF Very High Frequency	30 MHz - 300 MHz	10 - 1 m
UHF Ultra High Frequency	300 MHz - 3 GHz	1000 - 100 mm
SHF Super High Frequency	3 GHz - 30 GHz	100 - 10 mm

Space weather impact on radio wave propagation is closely related to the state of the geo-plasma, in particular the ionosphere, acting as propagation medium.

# Sounding the Ionosphere with radio waves



**ISR:** Radar utilizes scattering at charged particles in the ionosphere up to 1000 km height.

**VS:** Radar utilizes reflection of radio waves at the bottomside of the ionosphere

- Our knowledge about the ionosphere stems mainly from the analysis of ionospheric modifications of propagation parameters of radio waves:  
**amplitude, phase, signal delay, polarization**
- **On the other hand:** Knowledge of space weather related ionospheric conditions is needed to understand/predict the propagation of radio waves



# Terrestrial radio wave propagation (HF)

## Radio Blackouts

			GOES X-ray peak brightness by class and by flux*	Number of events when flux level was met; (number of storm days)
<b>R 5</b>	Extreme	<u>HF Radio:</u> Complete HF (high frequency**) radio blackout on the entire sunlit side of the Earth lasting for a number of hours. This results in no HF radio contact with mariners and en route aviators in this sector. <u>Navigation:</u> Low-frequency navigation signals used by maritime and general aviation systems experience outages on the sunlit side of the Earth for many hours, causing loss in positioning. Increased satellite navigation errors in positioning for several hours on the sunlit side of Earth, which may spread into the night side.	X20 ( $2 \times 10^{-3}$ )	Fewer than 1 per cycle
<b>R 4</b>	Severe	<u>HF Radio:</u> HF radio communication blackout on most of the sunlit side of Earth for one to two hours. HF radio contact lost during this time. <u>Navigation:</u> Outages of low-frequency navigation signals cause increased error in positioning for one to two hours. Minor disruptions of satellite navigation possible on the sunlit side of Earth.	X10 ( $10^{-3}$ )	8 per cycle (8 days per cycle)
<b>R 3</b>	Strong	<u>HF Radio:</u> Wide area blackout of HF radio communication, loss of radio contact for about an hour on sunlit side of Earth. <u>Navigation:</u> Low-frequency navigation signals degraded for about an hour.	X1 ( $10^{-4}$ )	175 per cycle (140 days per cycle)
<b>R 2</b>	Moderate	<u>HF Radio:</u> Limited blackout of HF radio communication on sunlit side of the Earth, loss of radio contact for tens of minutes. <u>Navigation:</u> Degradation of low-frequency navigation signals for tens of minutes.	M5 ( $5 \times 10^{-5}$ )	350 per cycle (300 days per cycle)
<b>R 1</b>	Minor	<u>HF Radio:</u> Weak or minor degradation of HF radio communication on sunlit side of the Earth, occasional loss of radio contact. <u>Navigation:</u> Low-frequency navigation signals degraded for brief intervals.	M1 ( $10^{-5}$ )	2000 per cycle (950 days per cycle)

\* Flux, measured in the 0.1-0.8 nm range, in  $\text{W m}^{-2}$ . Based on this measure, but other physical measures are also considered.

\*\* Other frequencies may also be affected by these conditions.

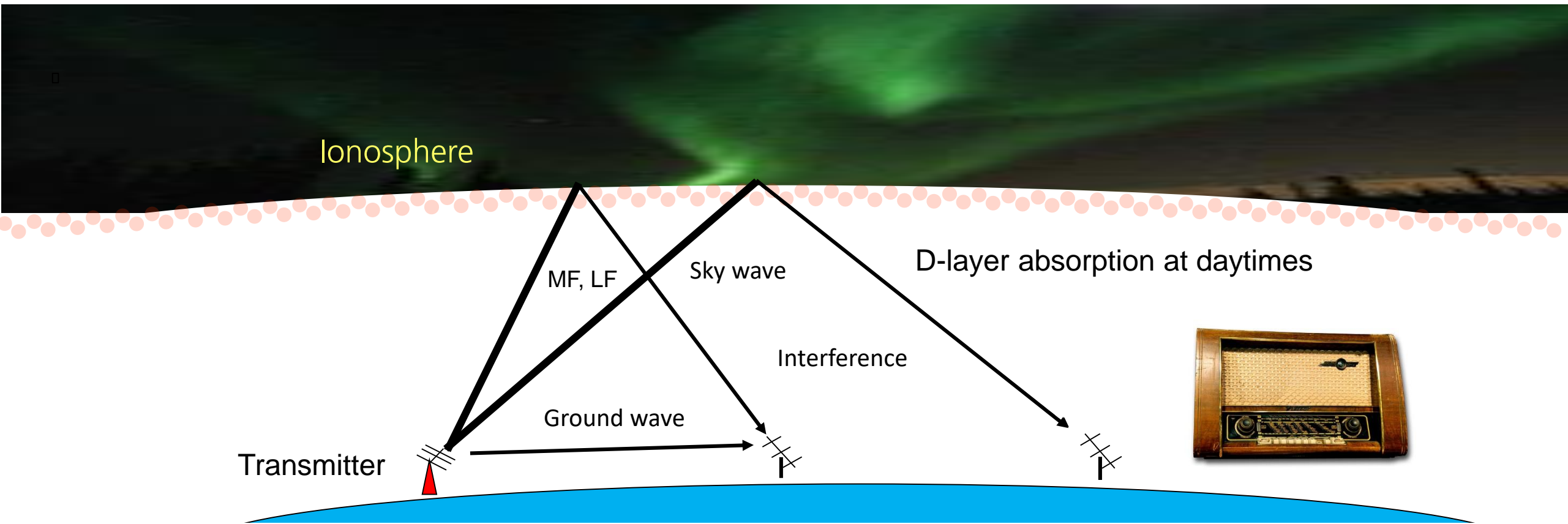
URL: [www.swpc.noaa.gov/NOAA\\_scales](http://www.swpc.noaa.gov/NOAA_scales)

April 1, 2011



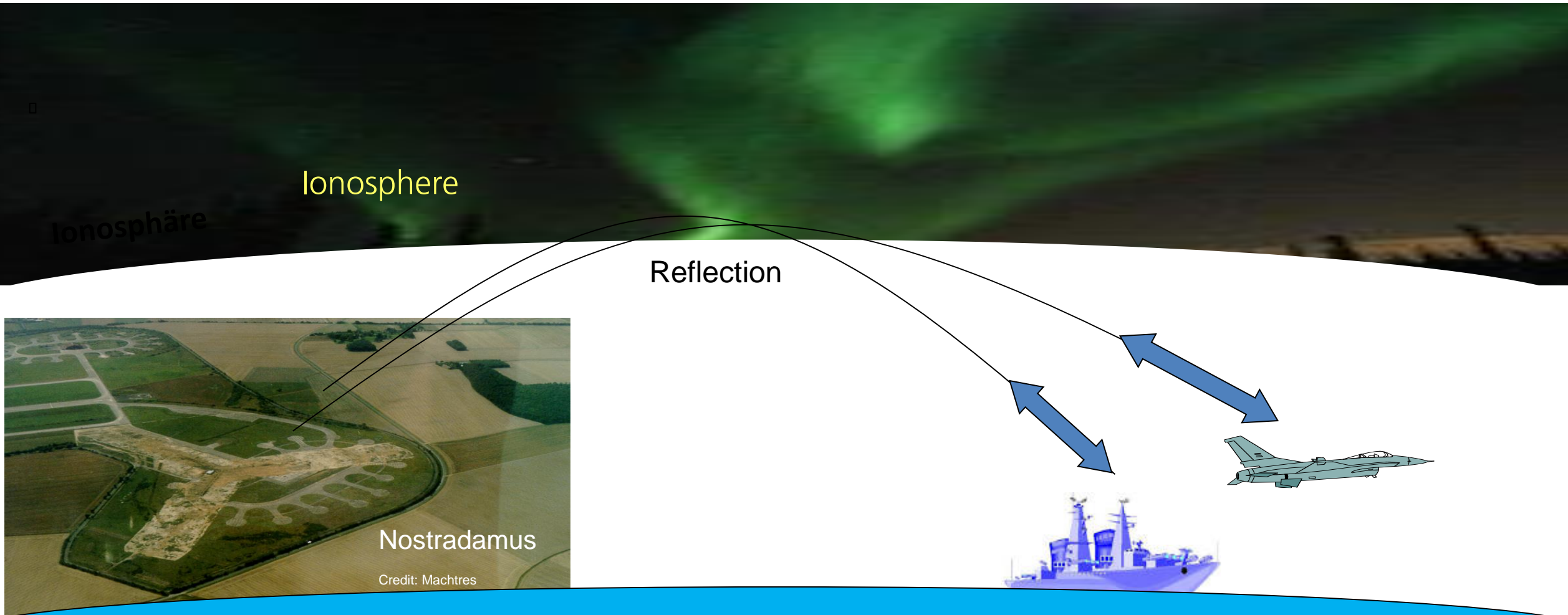


# Terrestrial radio wave propagation (HF)



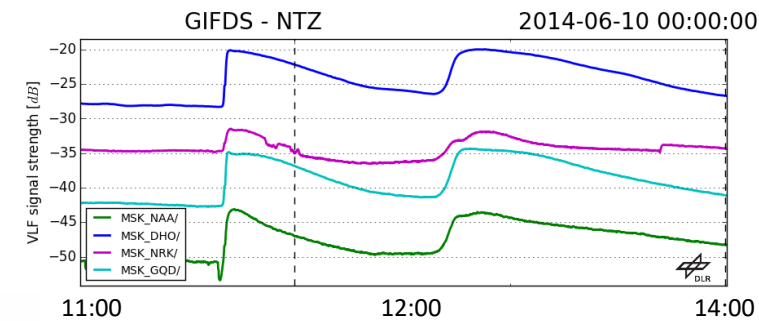
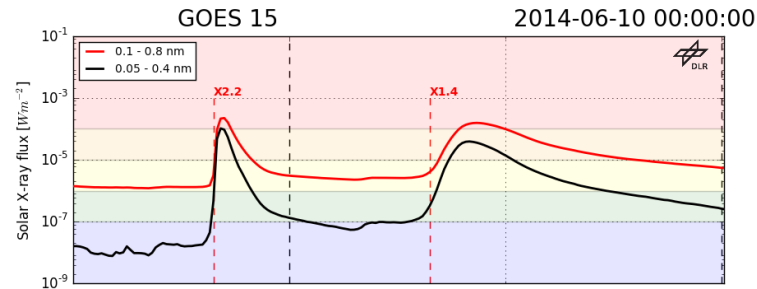
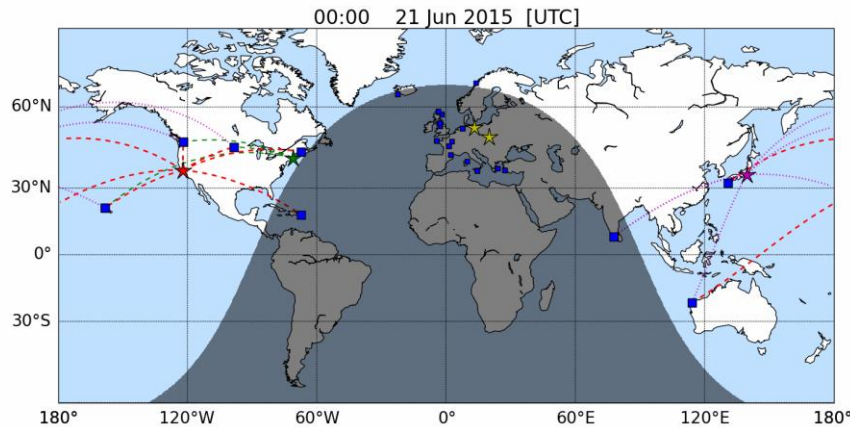
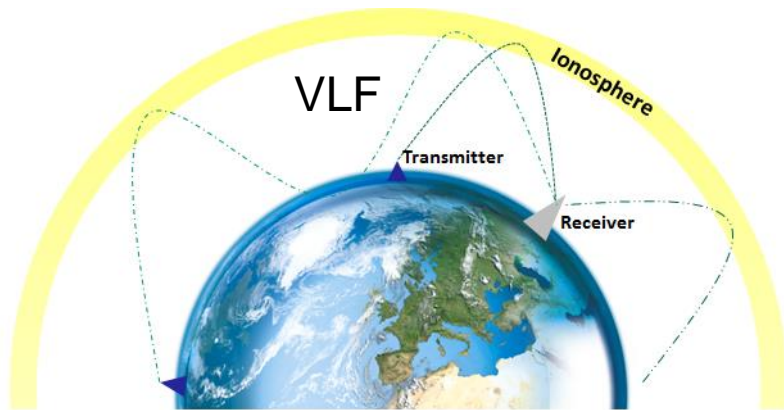
D-layer exists only at daytime created by the energetic spectrum of solar radiation reduces in particular the strength of MF and LF signals, phase shift of radio waves

# OTH - Radar NOSTRADAMUS near Paris



Nostradamus: 300 antennas, Range: 3000 km, f: 6-28 MHz, Detection of airplanes and ships, e.g. North Africa

# Solar Flare impact on VLF radio wave propagation (e.g. June 10, 2014)



GIFDS  
Global Ionosphere Flare Detection System



VLF receiver

Severe solar radiation bursts commonly measured as X ray bursts at GOES satellites may considerably enhance the plasma density in the ionosphere.

X rays: impact mainly the bottomside ionosphere, i.e. HF communication is affected.

EUV: impacts mainly the F2 layer, trans-ionospheric communication incl. GNSS applications are affected.

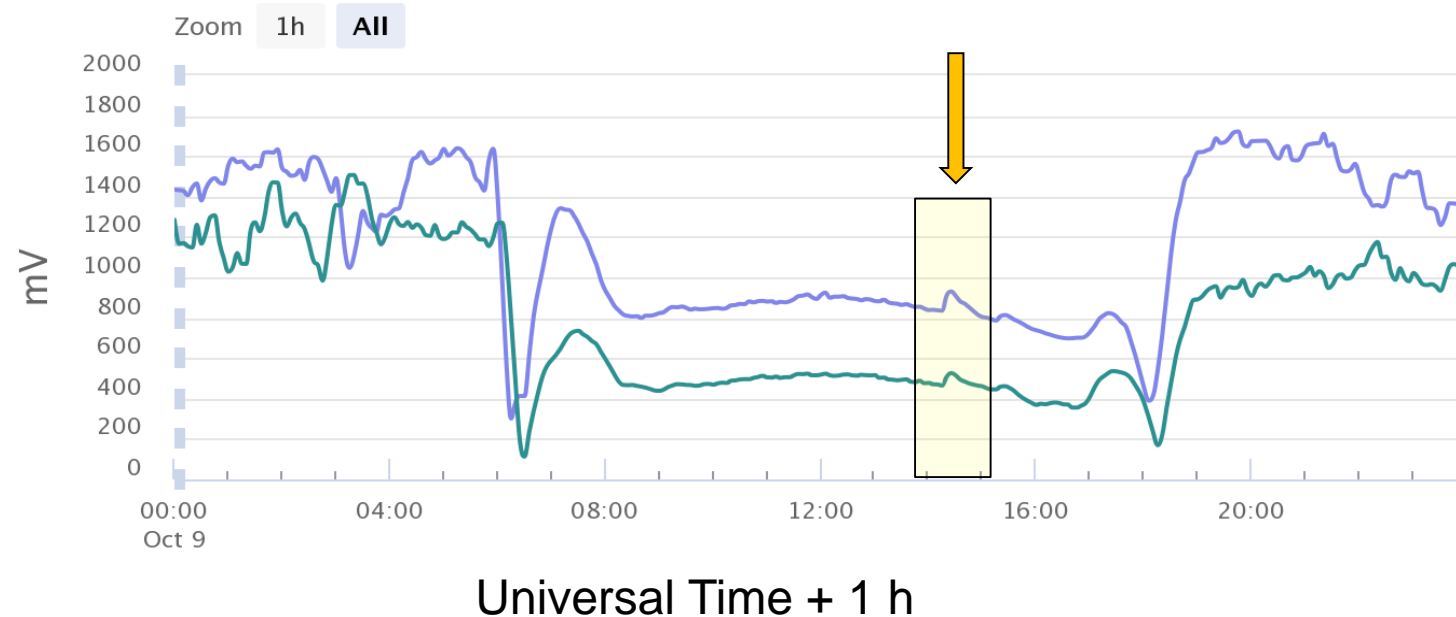
Wenzel et al. (2016) Global ionospheric flare detection system (GIFDS), JASTP, vol. 138-139, 233-242, <http://dx.doi.org/10.1016/j.jastp.2015.12.011>



# Detection of a Gamma ray burst on October 9, 2022 by students project SOFIE

## SOLar Flares by Ionospheric Effects (SOFIE)

<http://www.projectlab-neustrelitz.de/site/de/sofie.html>



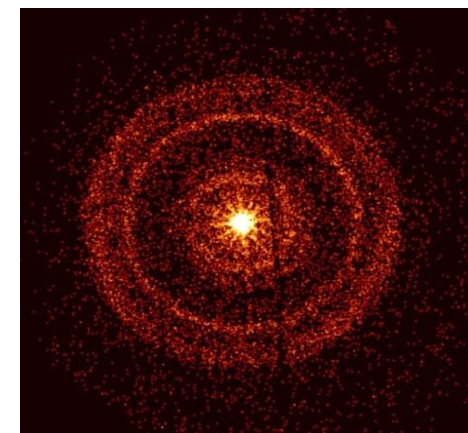
Amplitude change of VLF waves due to GRB enhanced ionization



Highcharts.com

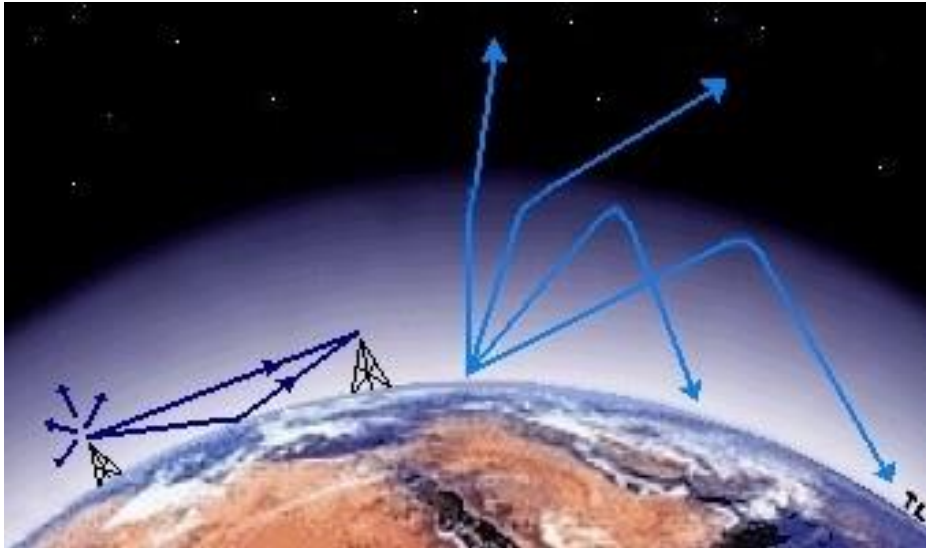
Long-lasting pulse of high-energy radiation that swept over Earth on Sunday, Oct. 9.

The emission came from a gamma-ray burst (GRB) – the most powerful class of explosions in the universe.

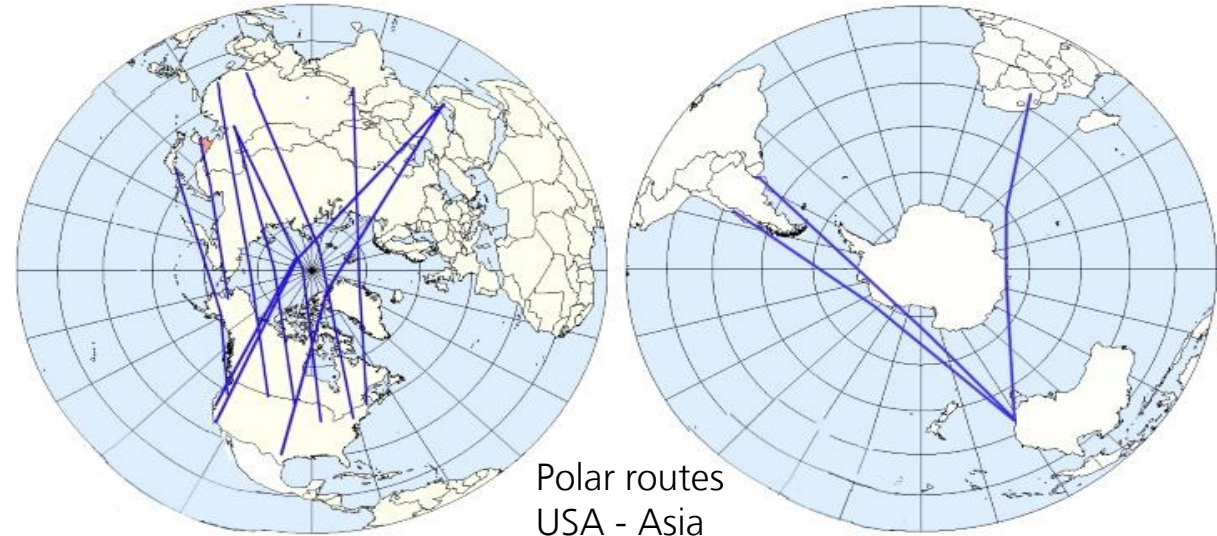


X ray light from GRB scattered by Milky Way dust  
Credit: NASA/Swift/A. Beardmore (University of Leicester)

# Space weather impact on terrestrial communication



- Radio waves at frequencies below 10 MHz are mostly reflected by the ionosphere
- Long distant propagation of waves possible, Maximum and Lowest usable frequency (MUF/LUF) information provided by HF services
- Solar flares and particle precipitation can prevent the ionosphere from reflecting radio waves (Short wave fadeout)



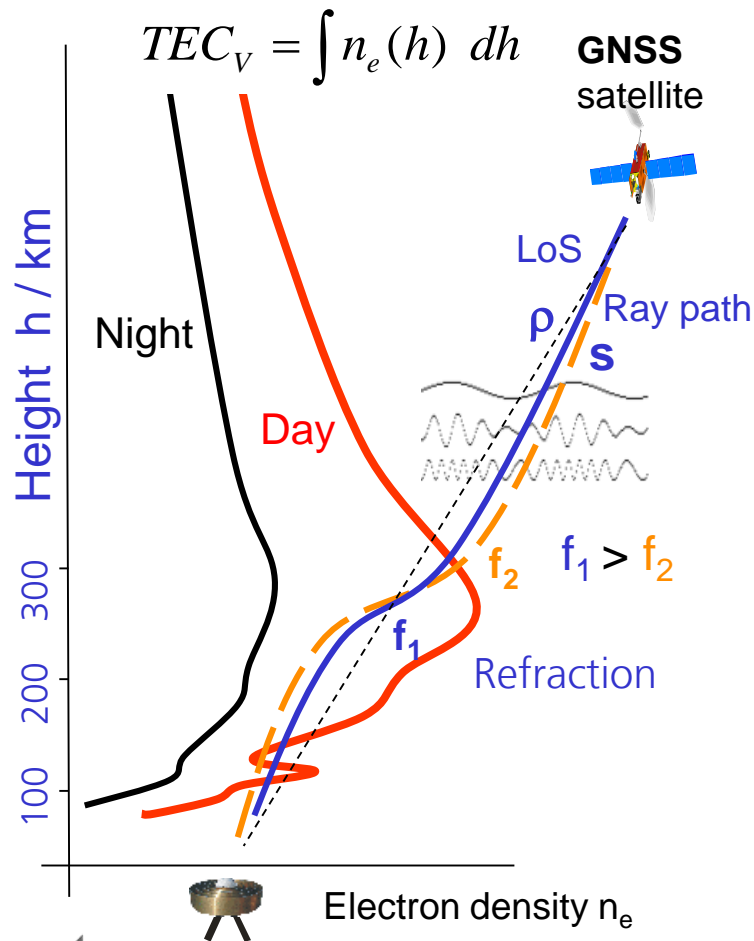
Polar routes  
USA - Asia

Source: Rolypolyman/Wikimedia Commons

- HF communication with airplanes may heavily be disturbed by ionospheric space weather effects (Fading, Blackout)
- Solar flares impact at day side preferrently at mid- to low latitudes
- Particle precipitation at high latitudes (aurora zone)
- Air traffic control in USA uses predictions concerning HF propagation risks from the Space Weather Prediction Center (SWPC) in Boulder / Colorado (NOAA scale)

# Trans-ionospheric propagation of radio waves

Focus on ranging: Space based navigation and remote sensing



Refraction of radio waves transmitted by satellites of Global Navigation Satellite Systems (GNSS):

The phase length  $L$  along the ray path  $s$  is defined by the integral

$$L = \int n ds = Min$$

where  $n$  is the refractive index and the integral becomes a minimum according to Fermat's principle of fastest arrival.

For GNSS, the phase length can be written:

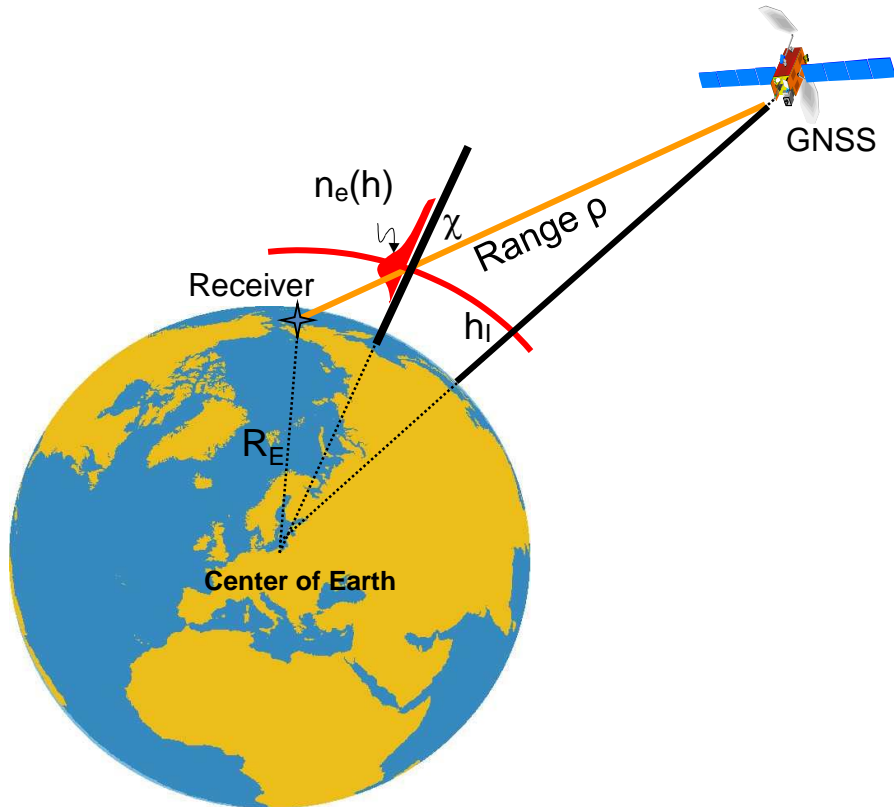
$$L = \int (n - 1) ds + \rho + \Delta s_B$$

where  $\rho$  is the line of sight and  $\Delta s_B$  means the excess path due to bending.





# Observation equations of GNSS measurements



Neglecting higher order terms in the refractive index and bending, the observation equations of GNSS measurements for code phases  $P_1/P_2$  and  $L_1/L_2$  carrier phases can be written:

Code  $P = \boxed{\rho} + c(\Delta t_{rec} - \Delta t^{sat}) + d_T \boxed{+ d_I} + d_{MP} + \varepsilon_P$

Carrier  $\Phi = \boxed{\rho} + c(\Delta t_{rec} - \Delta t^{sat}) + d_T \boxed{- d_I} + d_{MP} + N_a \lambda + \varepsilon_\Phi$

$\rho$	true range between GPS satellite and receiver along ray path s
$c$	velocity of light
$\Delta t^{sat}$	offset of satellite clock from GNSS Time
$\Delta t_{rec}$	offset of receiver clock from GNSS Time
$d_I$	<b>ionospheric phase delay along s</b>
$d_T$	atmospheric phase delay along s
$d_{MP}$	error due to multipath
$\lambda$	wave length of radio wave
$N_a$	phase ambiguity number (integer)
$\varepsilon$	Phase noise

$$d_I \approx \frac{K}{f^2} \cdot STEC$$

Ionospheric first order range error depends on the Total Electron Content along the slant ray path (STEC)

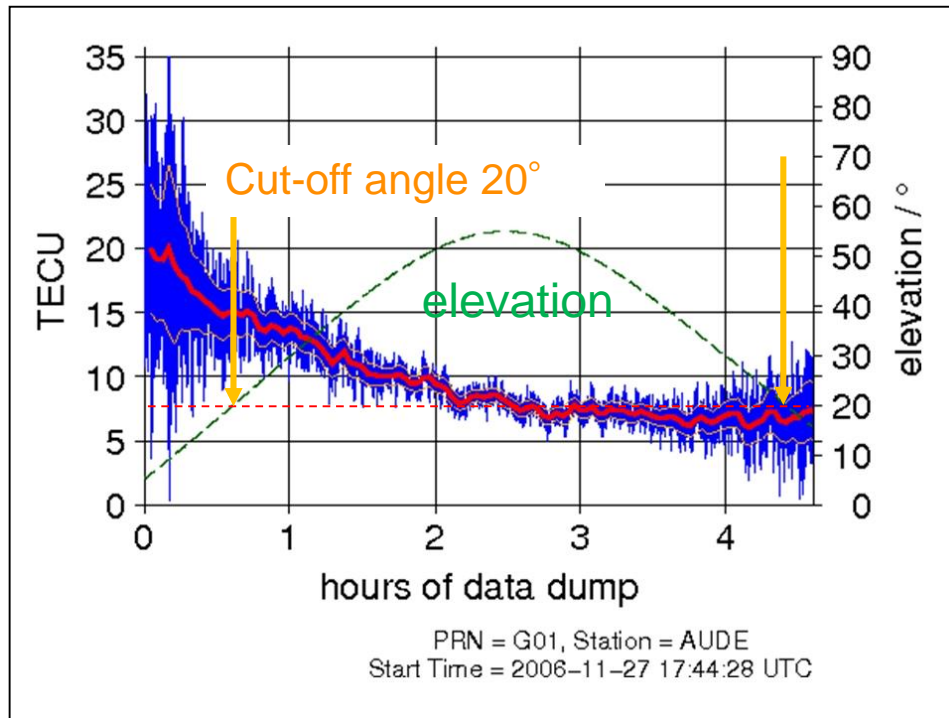
$$K = 40.3 \text{ m}^3 \text{s}^{-2}$$

$d_I$  up to 100 m

Differential code phase allows correcting  $d_I$

$$\Delta P = P_2 - P_1 = K \frac{f_1^2 - f_2^2}{f_1^2 f_2^2} STEC + \varepsilon_{off}$$

# Computation of the Total Electron Content (TEC)



1 TECU =  $10^{16}$  electrons /  $m^2 \approx 0.16m$  at  $L_1$  frequency

$$STEC = \frac{f_1^2 \cdot f_2^2}{K(f_1^2 - f_2^2)} (\Phi_1 - \Phi_2) + B + \varepsilon_N$$

Bias ←

$$P_2 - P_1 = \frac{K(f_1^2 - f_2^2)}{f_1^2 \cdot f_2^2} STEC + \varepsilon_{Poff}$$

$$\Phi_1 - \Phi_2 = \frac{K(f_1^2 - f_2^2)}{f_1^2 \cdot f_2^2} STEC + \varepsilon_{\Phi off}$$

$$K = 40.3 \text{ m}^3 \text{ s}^{-2}$$

GPS  $L_1 = 1575.42 \text{ MHz}$

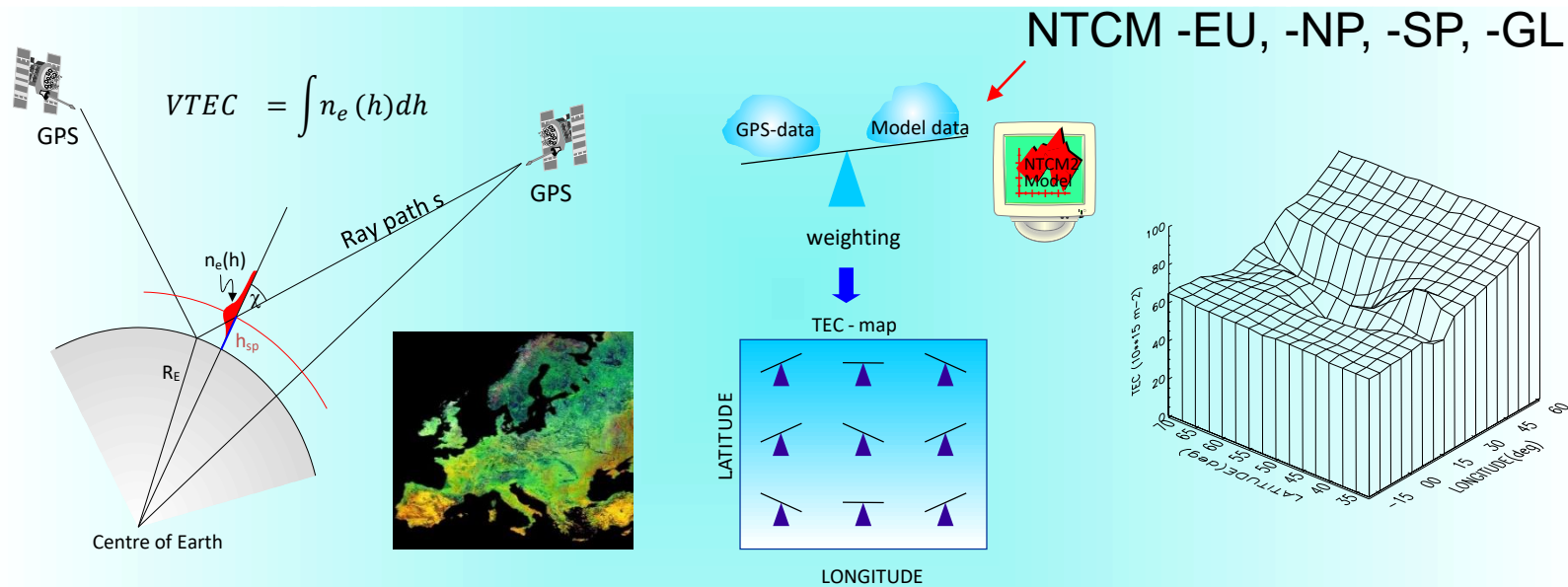
$L_2 = 1227.60 \text{ MHz}$

After levelling relative carrier phase differences into absolute uncalibrated code phase differences, subsequent TEC computation uses only carrier phases.

Jakowski, N. (1996). Modern Ionospheric Science, (Eds. H.Kohl, R. Rüster, K. Schlegel), EGS, Katlenburg-Lindau, ProduServ GmbH Verlagsservice, Berlin, pp 371-390

Jakowski, N. (2017). Ionosphere monitoring. In: Springer Handbook of Global Navigation Satellite Systems, Springer Verlag, 1139-1162. ISBN 978-3-319-429292-7.

# TEC monitoring for range error mitigation



Measurement,  
Calibration

Conversion  
to vertical

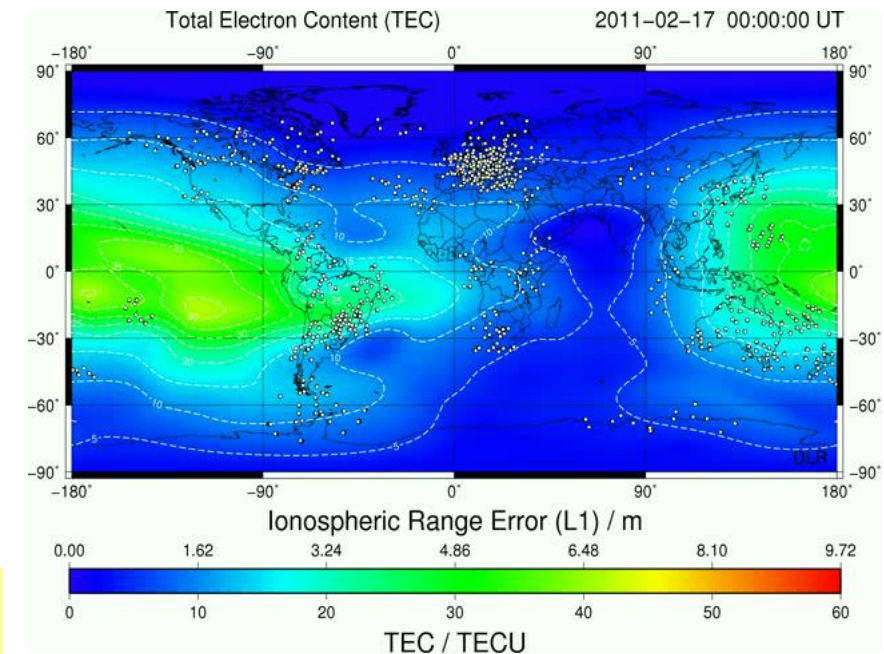
Data assimilation into a  
regional/global TEC model

TEC- Map

Jakowski, N., Modern Ionospheric Science, (Eds. H.Kohl, R. Rüster, K. Schlegel), EGS, Katlenburg-Lindau, ProduServ GmbH Verlagsservice, Berlin, pp 371-390,1996



## Global TEC map

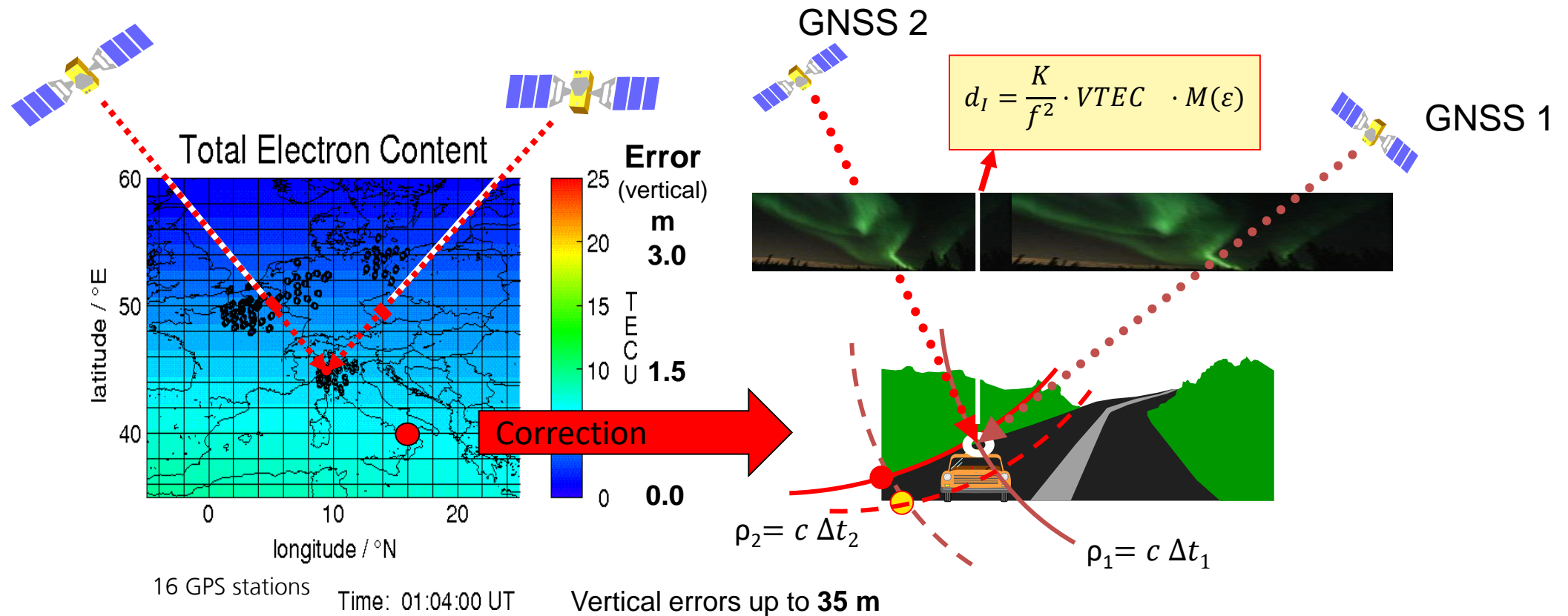


Background model:  
**Neustrelitz TEC Model (NTCM)**

Jakowski et al. (2011) A new global TEC model for estimating transionospheric radio wave propagation errors, Journal of Geodesy, 10.1007/s00190-011-0455-1



# Ionospheric range error correction for single frequency GNSS by n.r.t. service



Near real time TEC monitoring data can be used for correcting single frequency GNSS measurements. Data base provided by geodetic networks such as the International GNSS Service (IGS) and national networks.

# Ionospheric error mitigation in single frequency applications by ionospheric models

## GPS: Klobuchar model (ICA)

Klobuchar J. (1987) Ionospheric time-delay algorithm for single frequency GPS users. IEEE Trans Aerosp Electron Syst 23: 325–332.

## Galileo: NeQuick

Nava B, Coisson P, Radicella SM (2008) A new version of the NeQuick ionosphere electron density model. J Atmos Terr Phys 70(15):1856–1862.

<https://doi.org/10.1016/j.jastp.2008.01.015>

## Beidou: BeiDou Global Ionospheric delay correction Model (BDGIM)

Wang, N., Li, Z., Yuan, Y., Huo, X. (2021) Bei Dou Global Ionospheric delay correction Model (BDGIM), performance analysis during different levels of solar conditions GPS Solutions, 25:97, <https://doi.org/10.1007/s10291-021-01125-y>

Galileo alternative:

## Neustrelitz TEC Model-Global (NTCM-G) recommended by European GNSS Service Center

Hoque, M.M., Jakowski, N., Orús-Pérez, R. (2019) Fast ionospheric correction using Galileo Az coefficients and the NTCM model, GPS Solutions, 23:41, <https://doi.org/10.1007/s10291-019-0833-3>

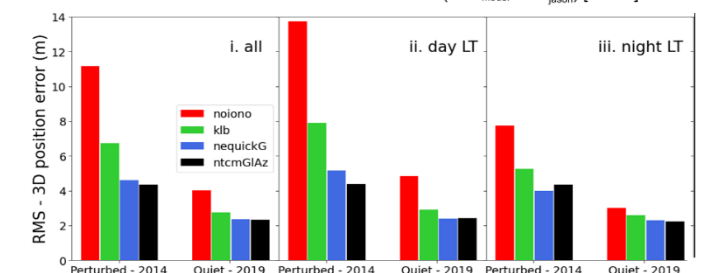
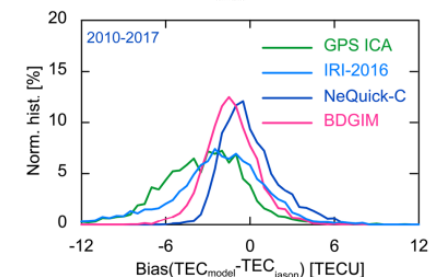
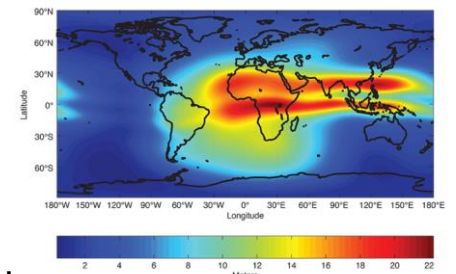
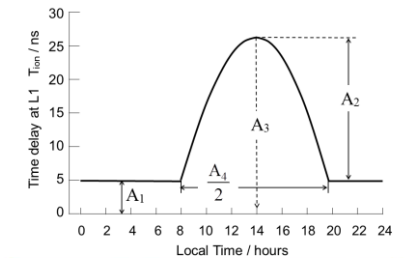
8 coefficients determine cosine type delay model of LT dependence  
Coefficients updated every day.

NeQuick 3D model of electron density, time consuming integration of electron density along ray paths.  
Virtual solar activity from updated Az

BeiDou Spherical Harmonics model of TEC, 9 model parameters are routinely updated using ionospheric observation and transmitted to single-frequency GNSS.

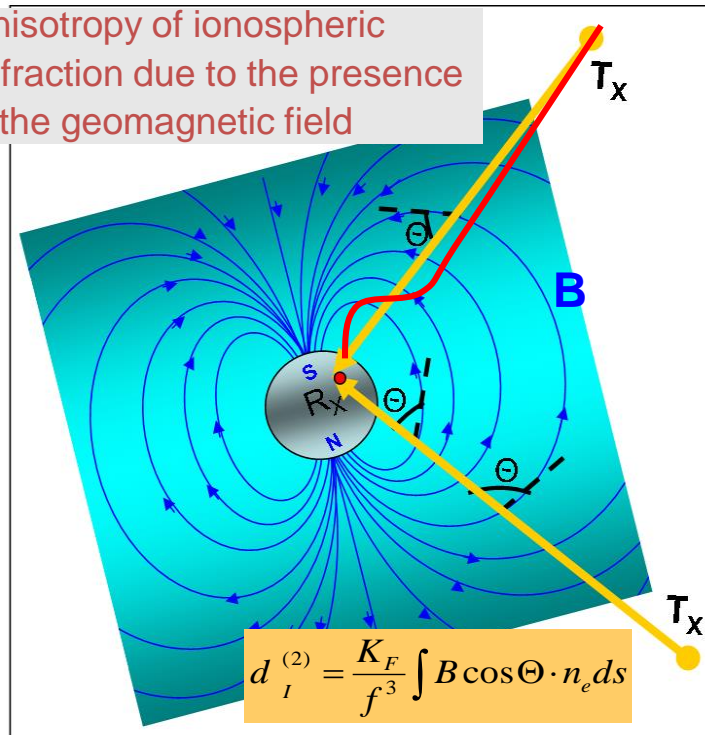
12 coefficients derived from NeQuick dedicated Az parameters.  
Compared with NeQuick very fast TEC or delay estimates

Accuracy of models < 80%



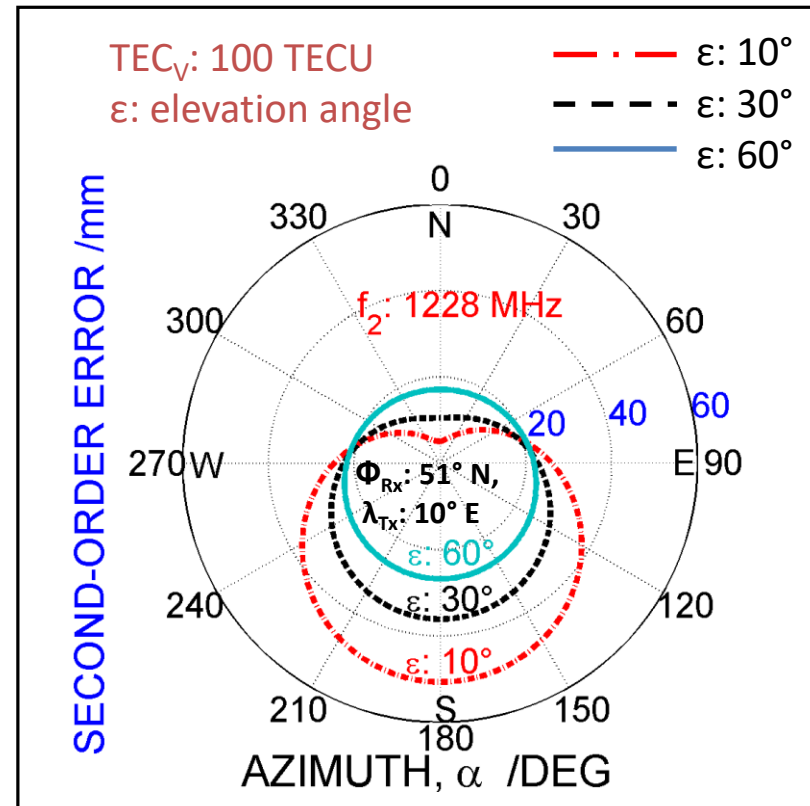
# Higher order refraction effects

Anisotropy of ionospheric refraction due to the presence of the geomagnetic field

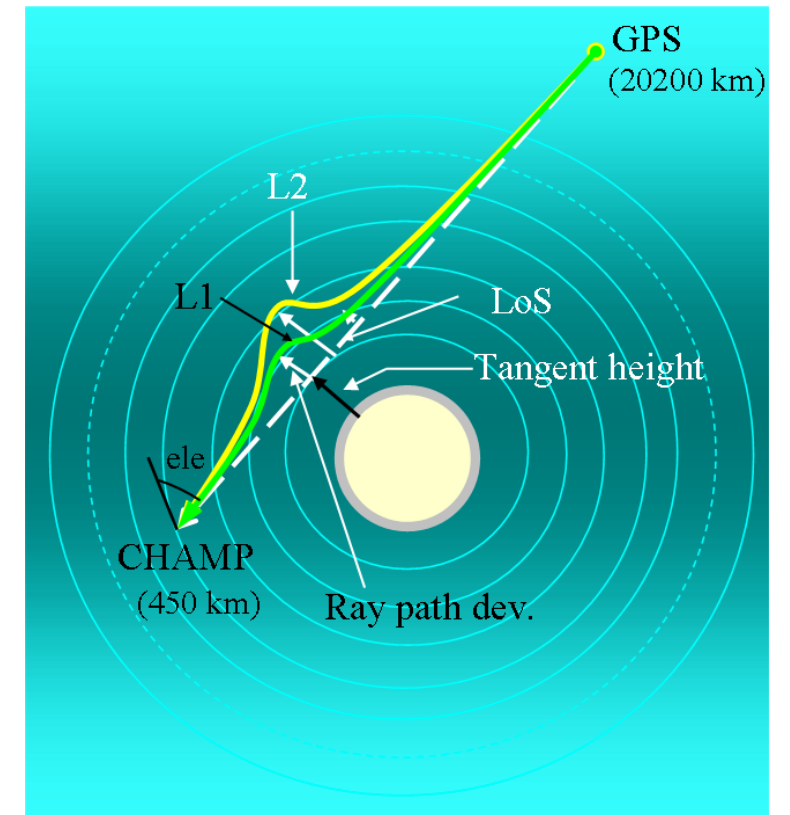


$$d_I^{(2)} = \frac{K_F}{f^3} \int B \cos \Theta \cdot n_e ds$$

- **Second order refraction error** (< 20 cm) mostly ignored
- **Correction:** possible via semiempirical formulas taking into account the regional link geometry



Hoque, M.M., N. Jakowski, Mitigation of higher order ionospheric effects on GNSS users in Europe, GPS Solutions, DOI 10.1007/s10291-007-0069-5, 2007



Ray path bending effect leads to an excess path length and error in tangential height estimation (up to 1 km between L1 and L2 ray paths)



# Ionosphere-free dual frequency linear combination

$$P = \boxed{\rho} + c(\Delta t_{rec} - \Delta t^{sat}) + d_T \boxed{+ d_I} + d_{MP} + \varepsilon_P$$

$$d_I \approx \frac{K}{f^2} \cdot STEC$$

$$\frac{f_1^2}{f_1^2 - f_2^2} P_1 - \frac{f_2^2}{f_1^2 - f_2^2} P_2 = \rho + \varepsilon_P$$

$d_I$  mitigated but higher order errors not

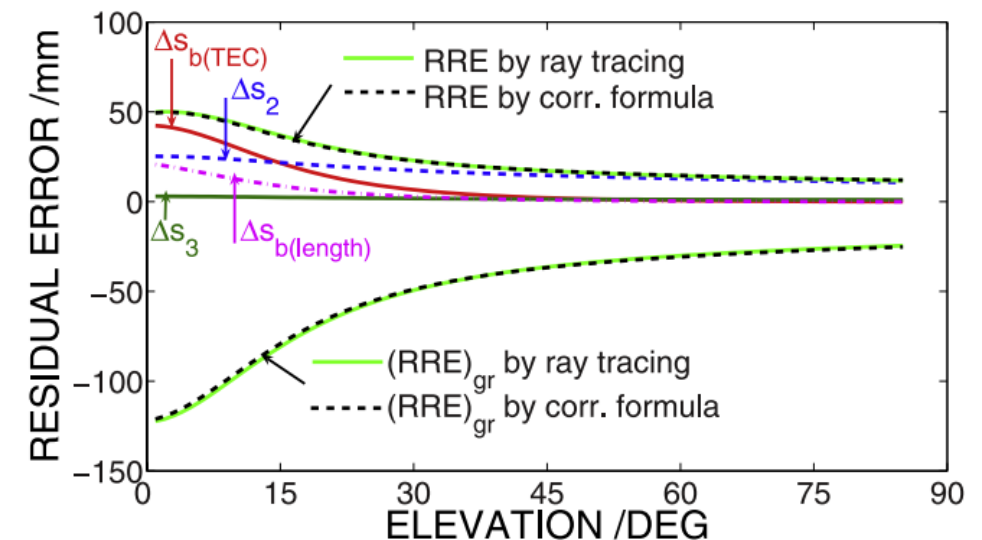
„ionosphere-free“ linear combination of L1 and L2 frequencies

This linear combination of two frequencies is able to mitigate the ionospheric range error by more than 99%.

Highest accuracy is achieved in Differential GNSS networks utilizing carrier phases.

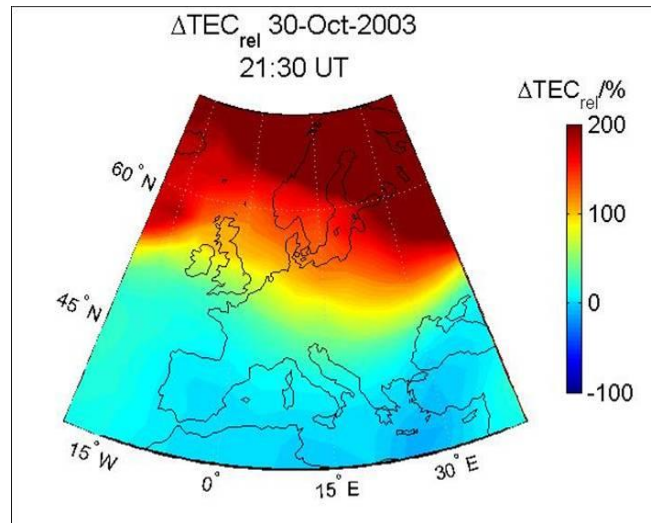
Dual frequency suffer in particular from ionospheric perturbations during ionospheric storms and from small scale plasma irregularities generating scintillations of amplitude and phase of radio waves.

Ionospheric residual range errors for GPS measurements.

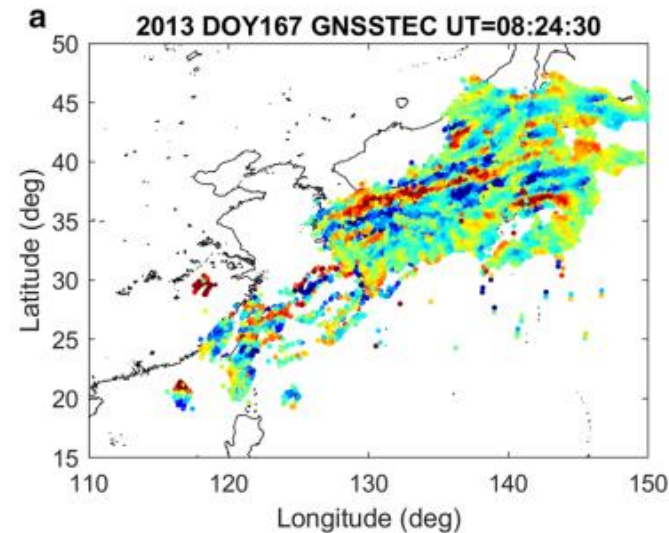


Hoque M. M. and N. Jakowski (2008), Estimate of higher order ionospheric errors in GNSS positioning, Radio Sci., 43, RS5008, doi: 10.1029/2007RS003817.

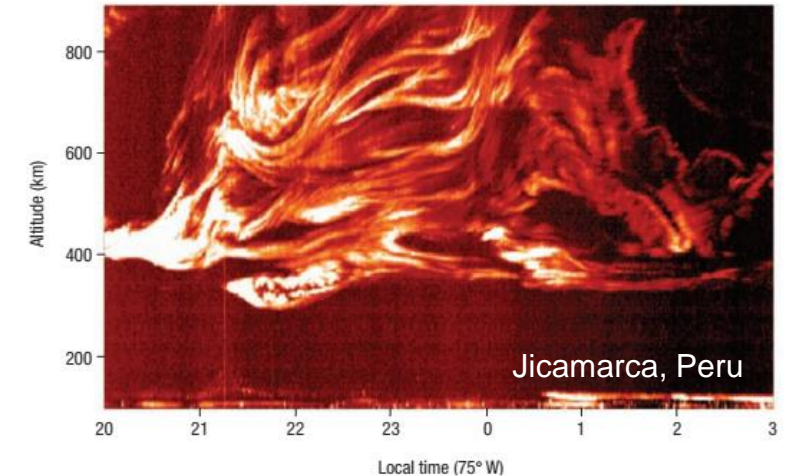
# Ionospheric perturbation types impacting ionospheric radio wave propagation



N. Jakowski et al. (2012): J. Space Weather and Space Clim., 2, A22.



Cheng et al. Earth, Planets and Space (2021) 73:105  
<https://doi.org/10.1186/s40623-021-01432-1>



M. Kelley (2008) nature geoscience | VOL 1 |  
FEBRUARY 2008 | [www.nature.com/naturegeoscience](http://www.nature.com/naturegeoscience)

## Large scale

Spatial/temp.scale:  $\approx 1000$  km/ hours  
Amp.: up to 250 TECU, Velocity:  $\approx 600$  m/s  
Moving ionization fronts, patches (LSTIDs)

How to characterize ionospheric perturbations?

In analogy to characterizing solar and geomagnetic activity (e.g. by F10 or Kp) ionospheric perturbations may be characterized also by indices that describe effects of ionospheric perturbations statistically.

## Mid-scale

Spatial/temp. scale:  $\approx 100$ -400km/min.  
Amp.:  $< \approx 1$  TECU, Velocity:  $\approx 100$ -250 m/s  
Wavelike plasma motion (MSTIDs)

## Small scale

Spatial/temp. scale:  $\leq 10$  km / seconds  
signal fading 20dB, Velocity:  $\approx 100$ -200 m/s  
Plasma turbulences, instabilities

e.g.

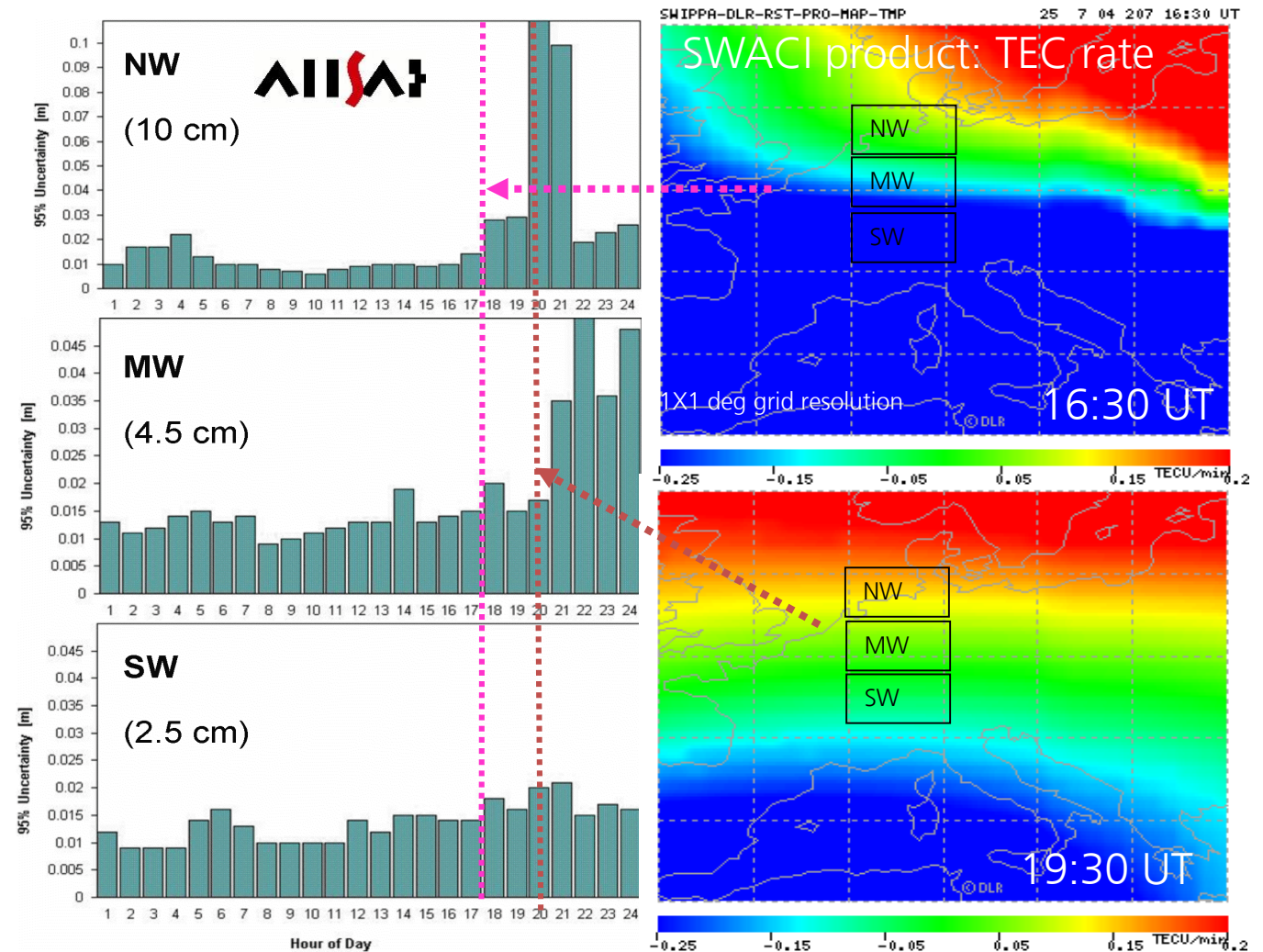
$S4$ ,  $\sigma_\phi$ ,  $ROT$ ,  $ROTI$ ,  
 $\Delta TEC$ ,  $GIX$ ,  $SIDX$

# Performance degradation of ascos GPS reference network (25 July 2004)

Performance of the GPS reference network of Allsat GmbH, Hannover degrades during the ionospheric storm on 25 July 2004

Different effects in different network areas over Germany

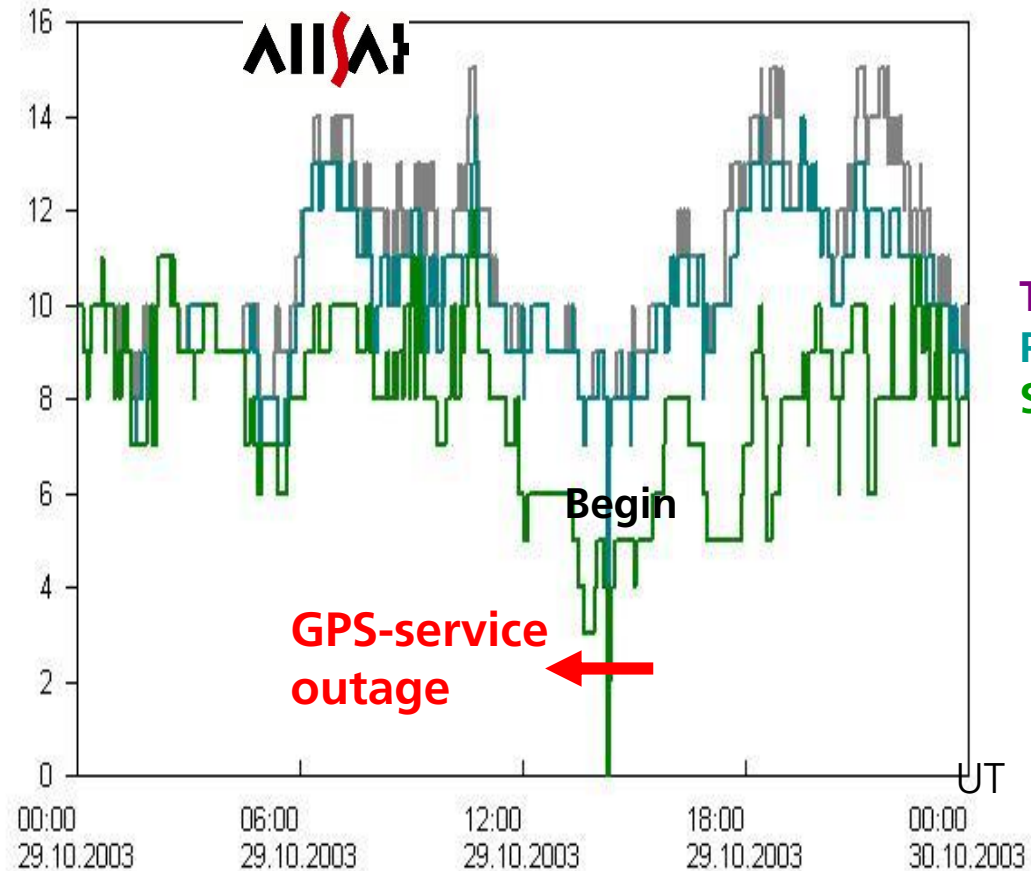
- Propagation of perturbation from high to mid-latitudes
- Provision of ionospheric now- and forecast information valuable for users
- Perturbation degree should be quantified by a perturbation index that can directly be used by customers



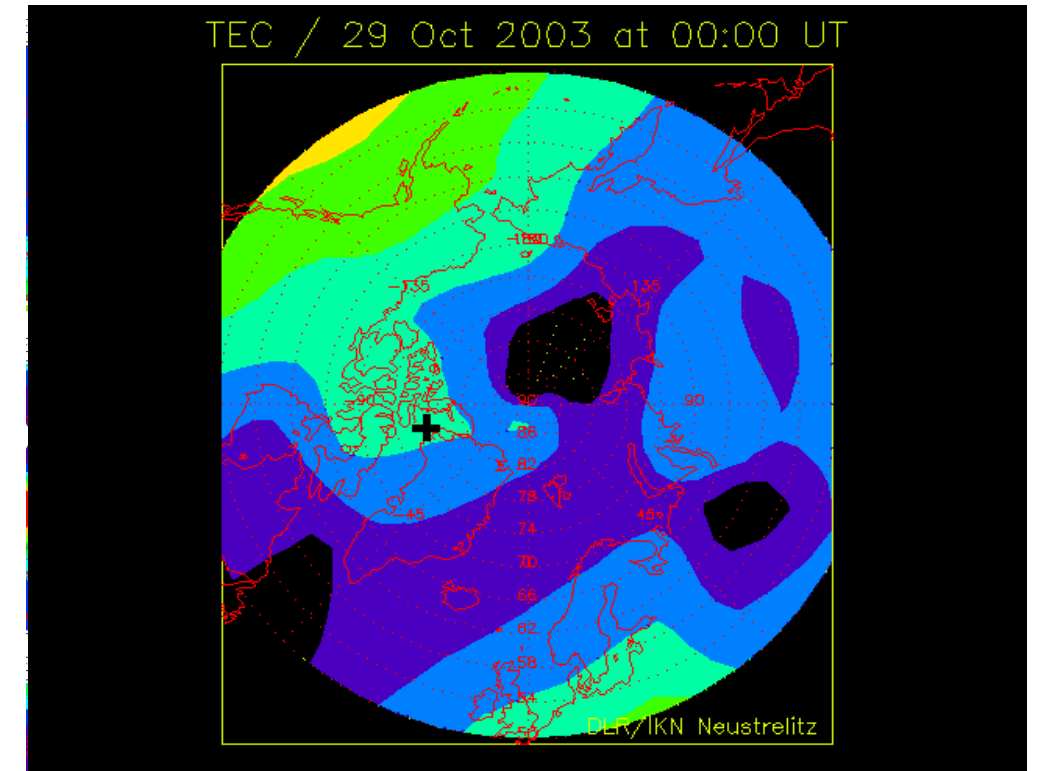


# Geomagnetic / ionospheric storm on October 29, 2003

## Performance of the ascos reference network



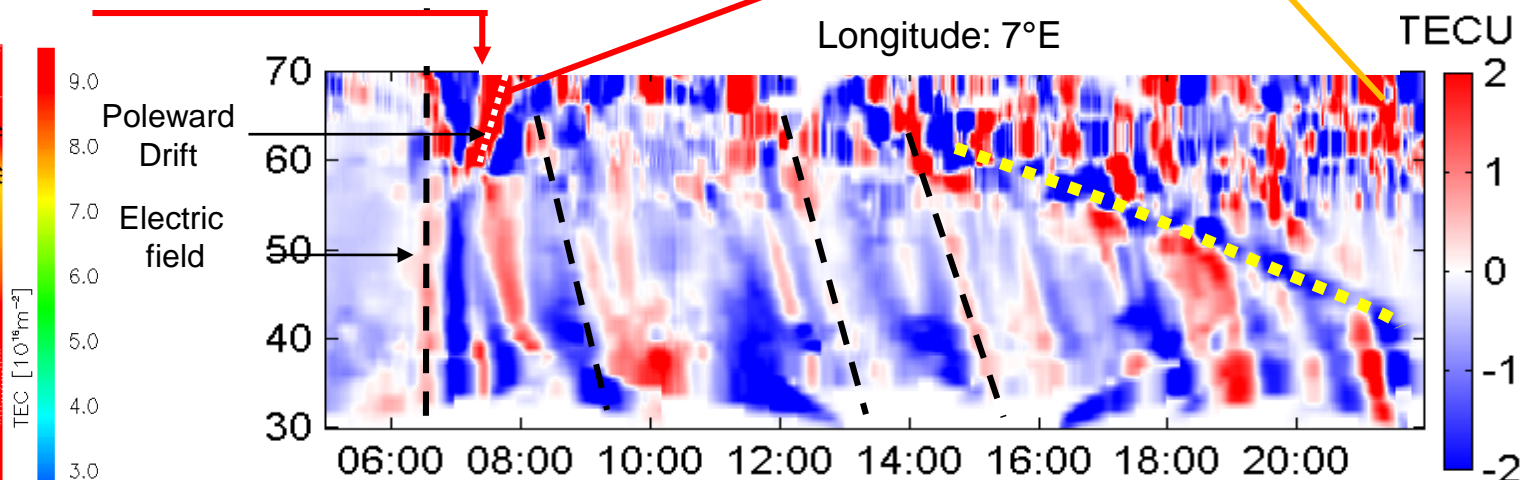
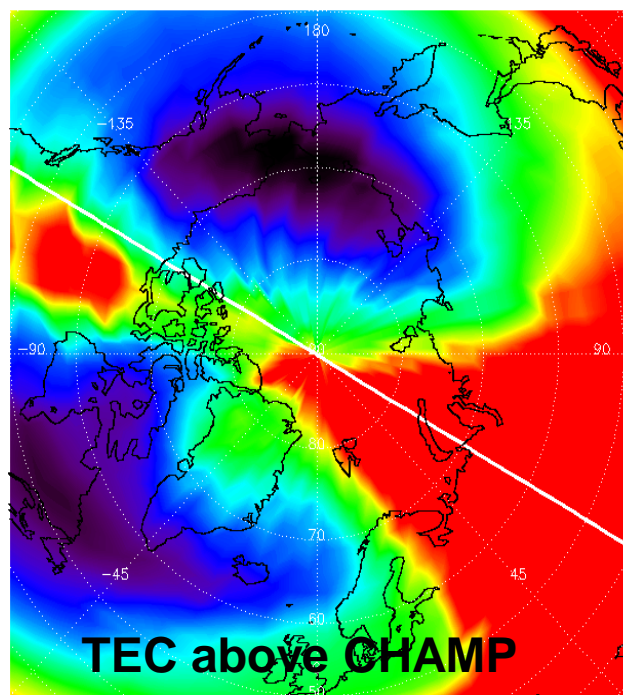
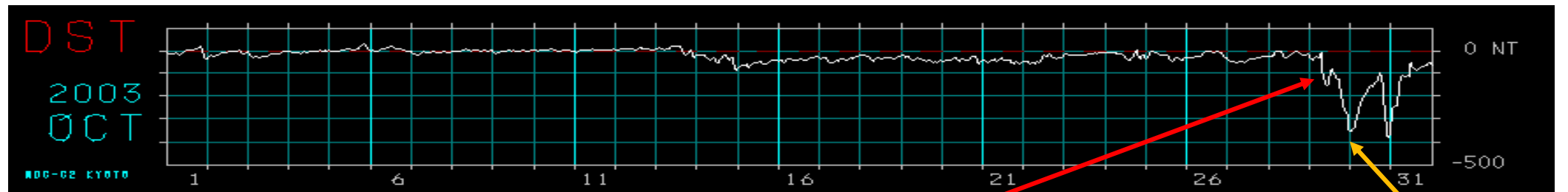
## Polar TEC map



$\Delta\text{TEC}=10\text{min}$



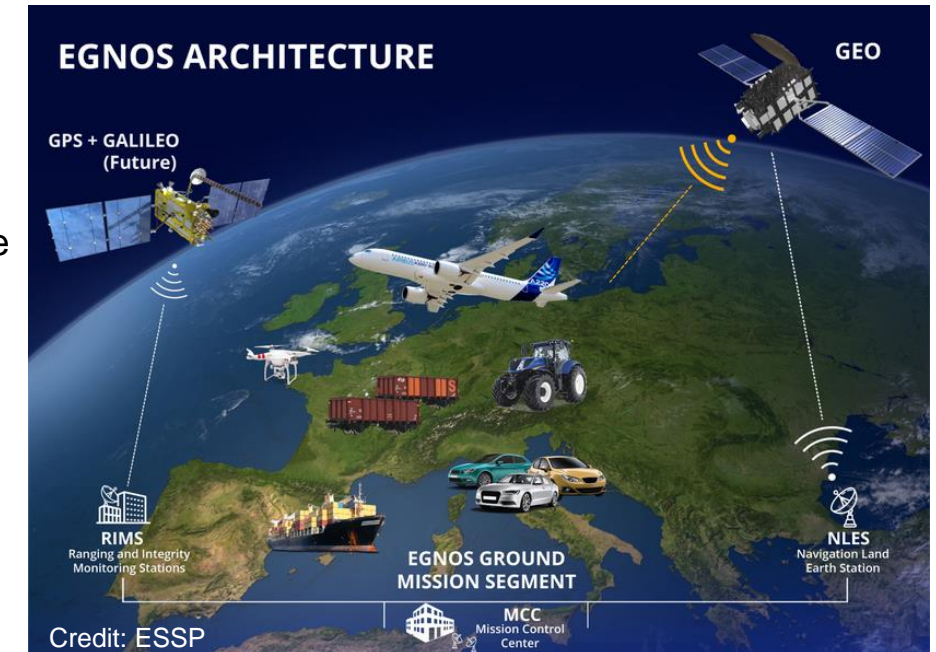
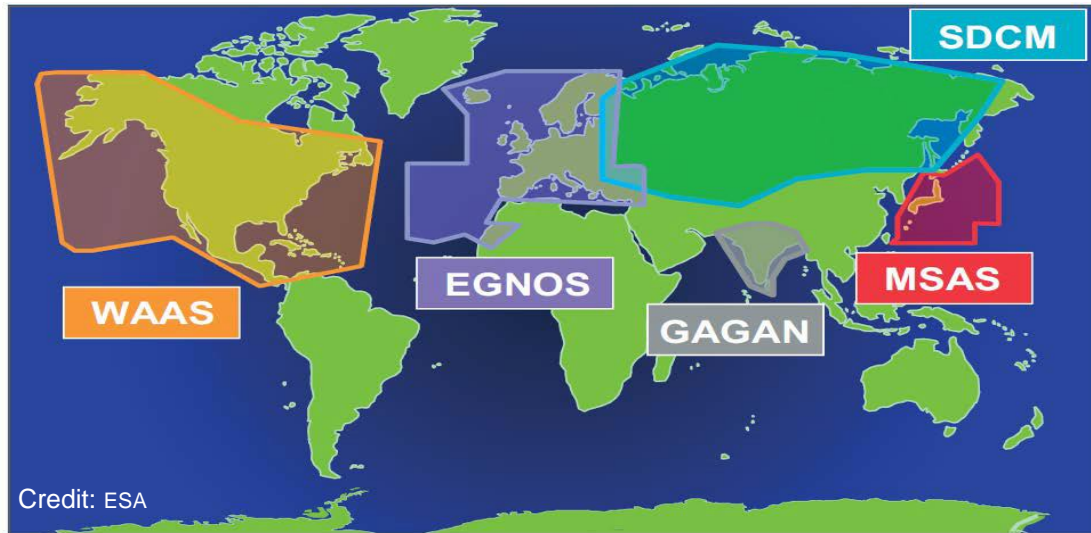
# Ionospheric storm generation and propagation



- Immediate response at all latitudes at storm onset
- Tongue of ionization across the Pole
- [Wavelike propagation of disturbances](#) during the main phase
- High latitude disturbance zone (northward of the trough) moves equatorward

Jakowski, et al. (2012). Monitoring, tracking and forecasting ionospheric perturbations using GNSS techniques, J. Space Weather Space Clim. 2 (2012) A22, DOI:10.1051/swsc/2012022

# Space Based Augmentation Systems (SBAS) in aviation



- WAAS (US): Wide Area Augmentation System; since 2003
- EGNOS (Europe): European Geostationary Overlay System; 2009
- MSAS (Japan): Multi-functional Satellite Augmentation System; 2007
- GAGAN (India): GPS Aided Geo Augmented Navigation
- SDCM (Russia): System of Differential Correction and Monitoring

Ground and space based augmentation systems (GBAS/SBAS) are needed to provide ionospheric range error corrections to airplanes.

Airplane navigation systems are allowed to use only the certified L1 GPS frequency.

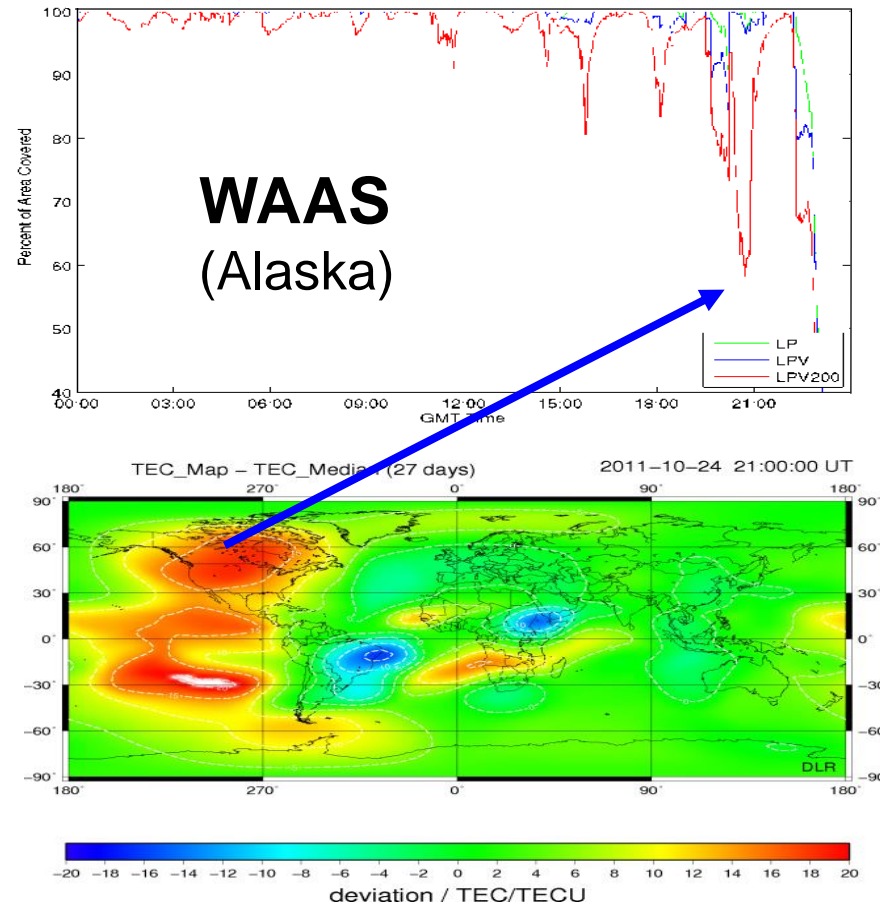
Implemented correction models are not reliable.



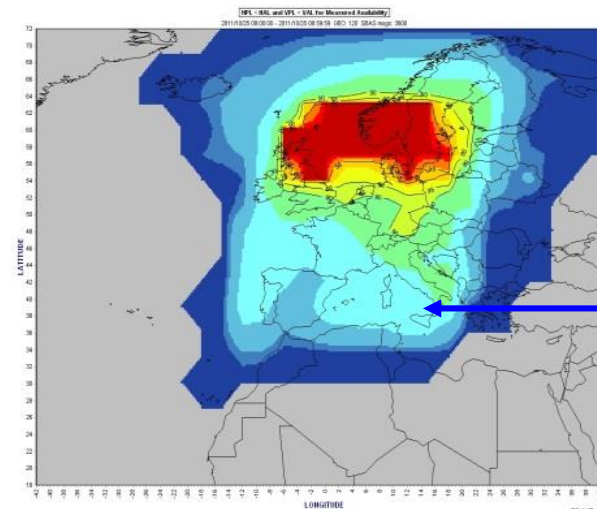
# Ionospheric impact on SBAS (WAAS/EGNOS) on 24/25 October 2011

25/10/2011 - 09:00UT

24/10/2011 - 21:00 UT

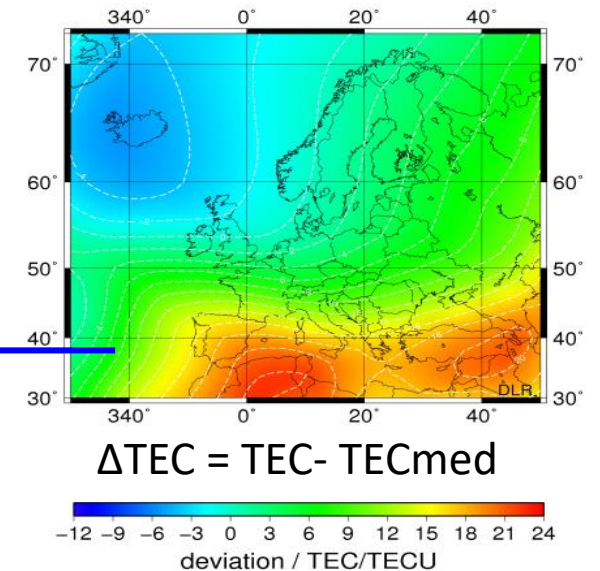


**EGNOS**



TEC\_Map - TEC\_Median (27 days)

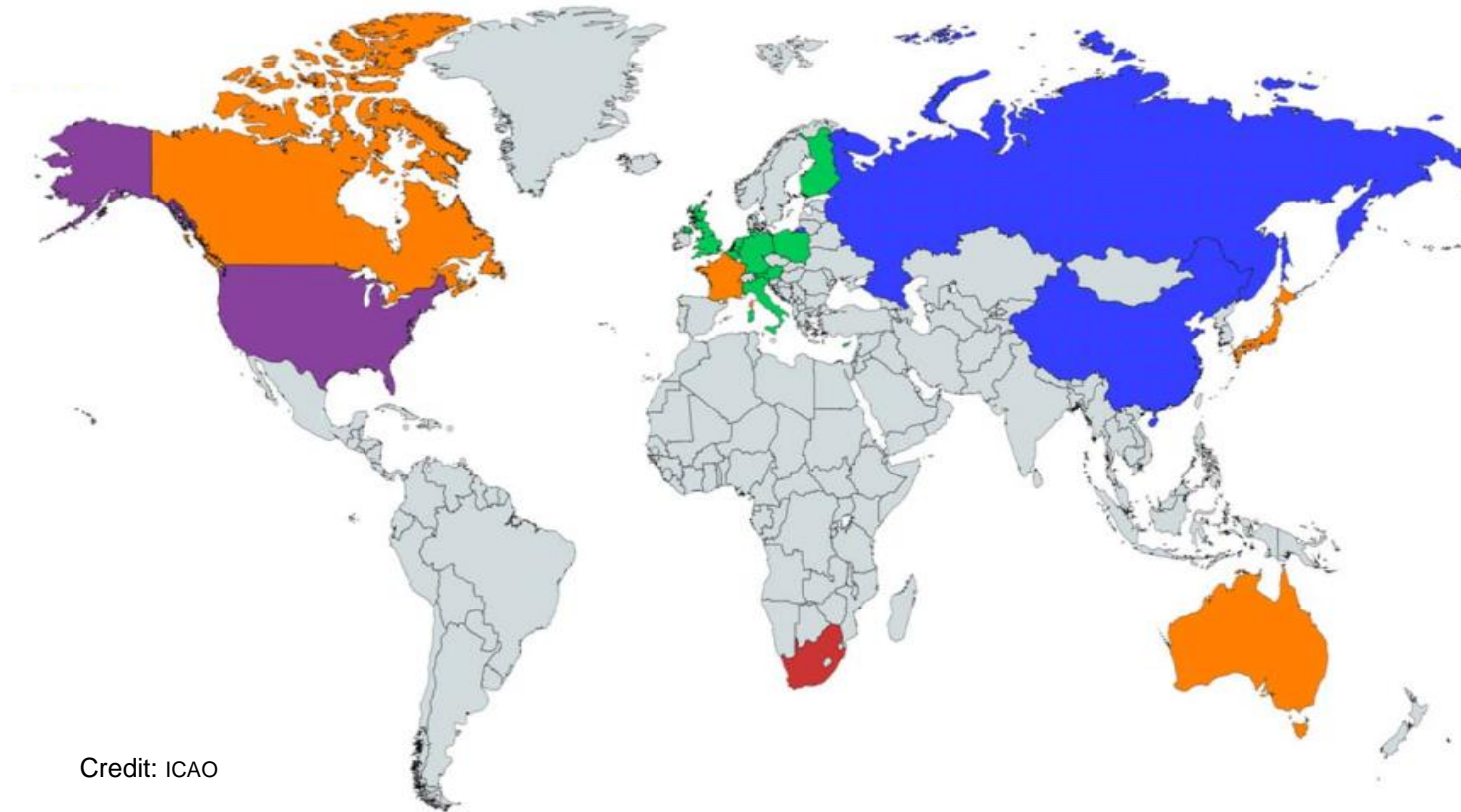
2011-10-25 09:00:00 UT



Ionospheric storm on October 25, 2011 causes strong deviations of TEC from average values (27 medians)

Performance of space based augmentation systems such as WAAS und EGNOS is strongly affected by ionospheric perturbations during the ionospheric storm.

# Designated ICAO Space Weather Centers



Credit: ICAO

- PECASUS (European consortium)
- ACFJ (Australia, Canada, France, Japan)
- NOAA SWPC (United States)
- China/Russia Consortium

Regional - South Africa

Tasks:

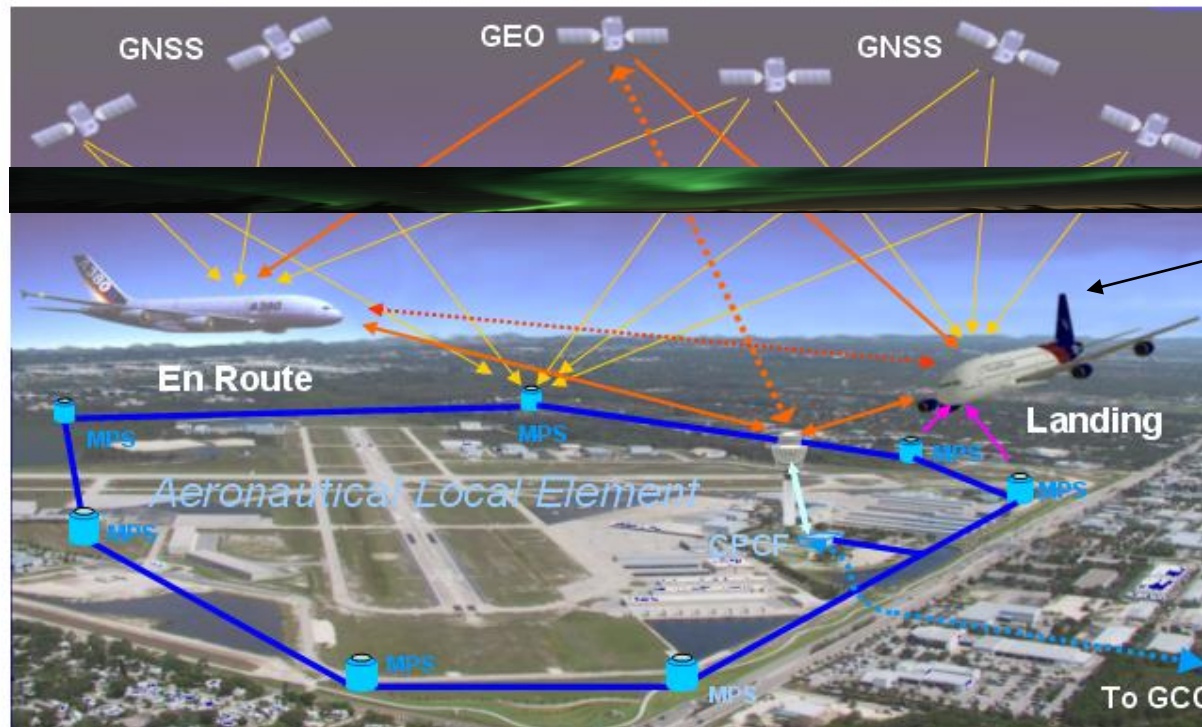
Development of specific space weather services relevant to aviation  
Nowcasting and forecasting capabilities

SW impact on

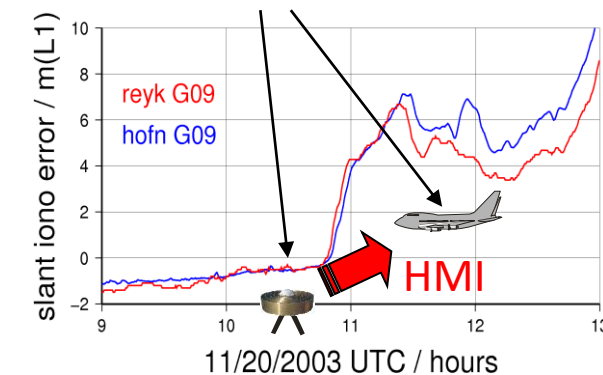
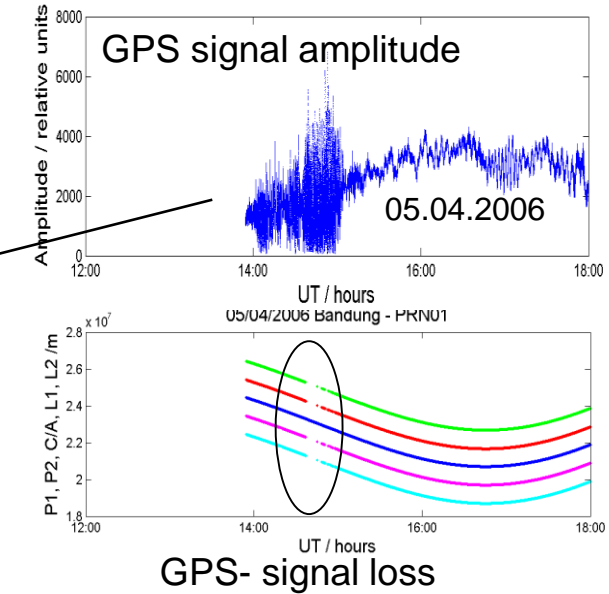
- HF communication
- GNSS navigation
- Radiation exposition at flights



# Ionospheric impact on GBAS - Safety of Life (SoL) application



- Degradation of accuracy, integrity, availability and continuity of signals due to space weather events
  - HF Communication disturbed or interrupted
- Operational detection and modelling of ionospheric perturbations needed
- Ionospheric "Threat-Model" required



**HMI:**  
Hazardous  
Misleading  
Information

Mayer, C. et al. (2009) Ionosphere Threat Space Model Assessment for GBAS. ION GNSS 2009, 22.-25. Sep. 2009, Savannah, GA, USA.



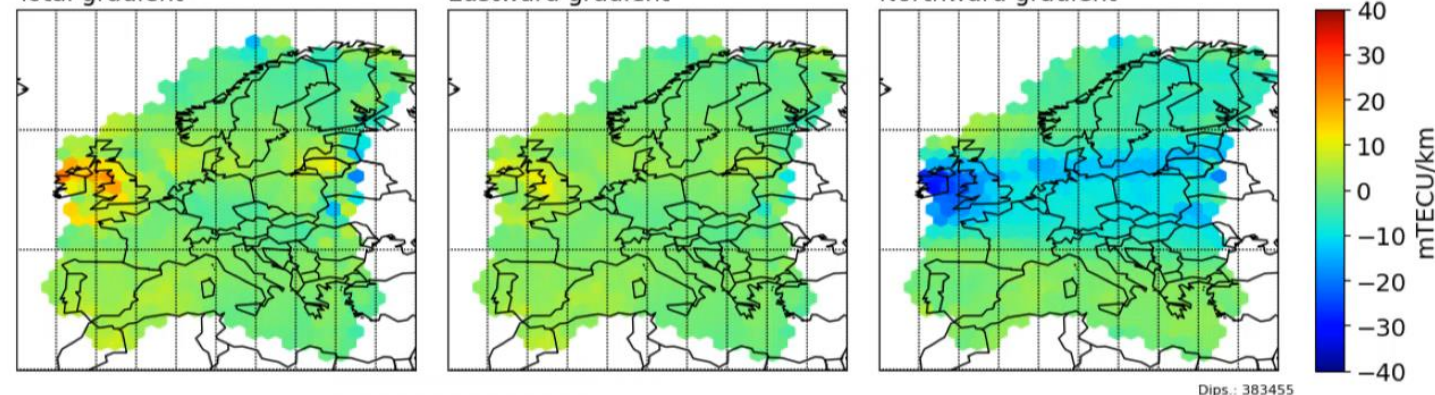
# TEC gradients (GIX) over Europe during the St. Patrick's Day storm March 2015

St. Patrick's Day storm (2015, DoY 076)

Total gradient

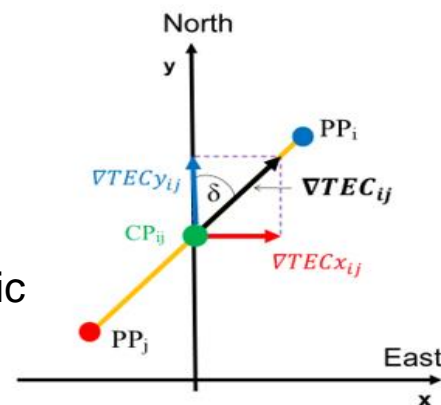
Eastward gradient

Time: 12h00m00s  
Northward gradient



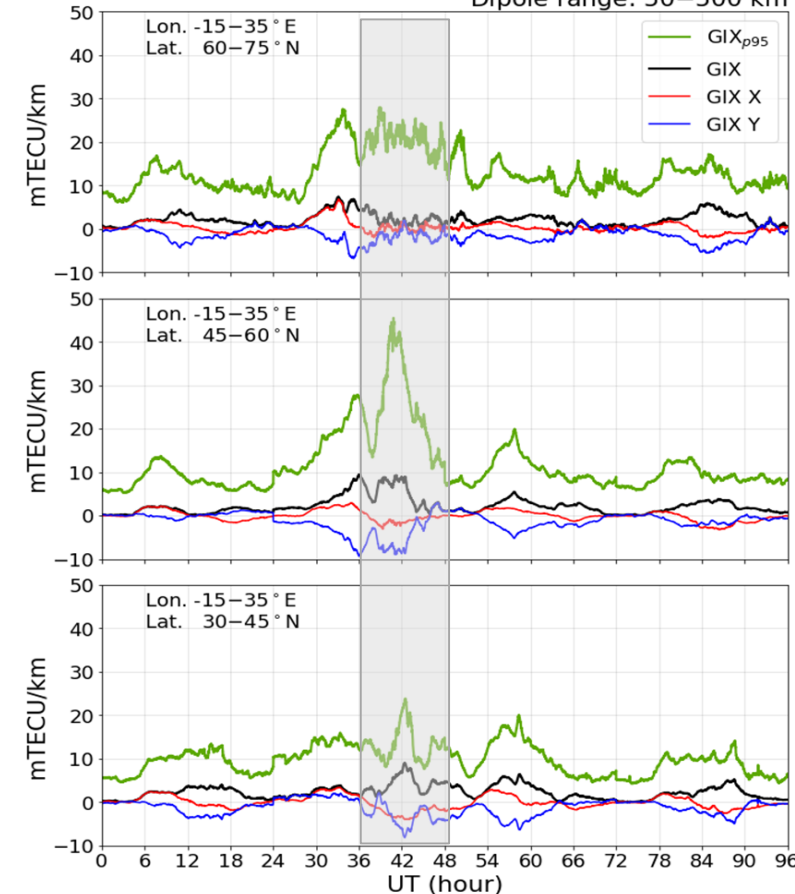
Dips.: 383455

- Spatial gradients calculated with a sample of 831 GNSS stations
- Time resolution of 30 s
- Dipole length ranges between 50 and 1000 km
- TEC gradient between ionospheric piercing points  $PP_i$  and  $PP_j$
- Averaging over all PPs at each epoch possible, i.e., instantaneous characterisation of ionospheric perturbation degree possible.



GIX St. Patrick's Day storm (DoY 075–078, 2015)

Dipole range: 50–500 km



Cahuasqui et al. (2022). Regional characterization of ionospheric perturbations degree with GIX and SIDX, 44th COSPAR Scientific Assembly, 16-24 Jul 2022, Athens, Greece.

# Space Weather Impact on GNSS – Solar Flare (SIDX)

## Sudden Ionospheric Disturbance index (SIDX)

## SIDX

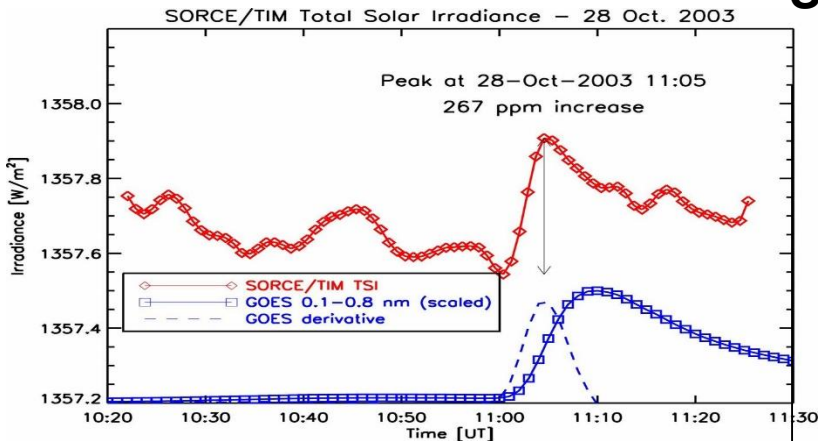
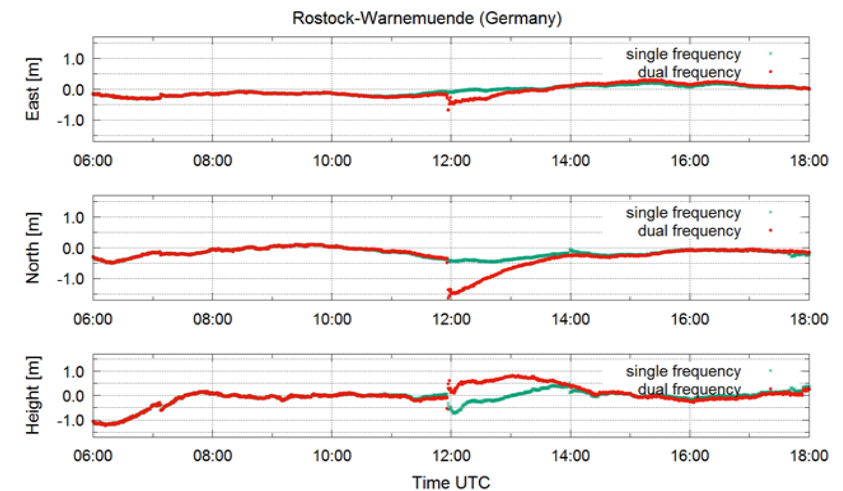
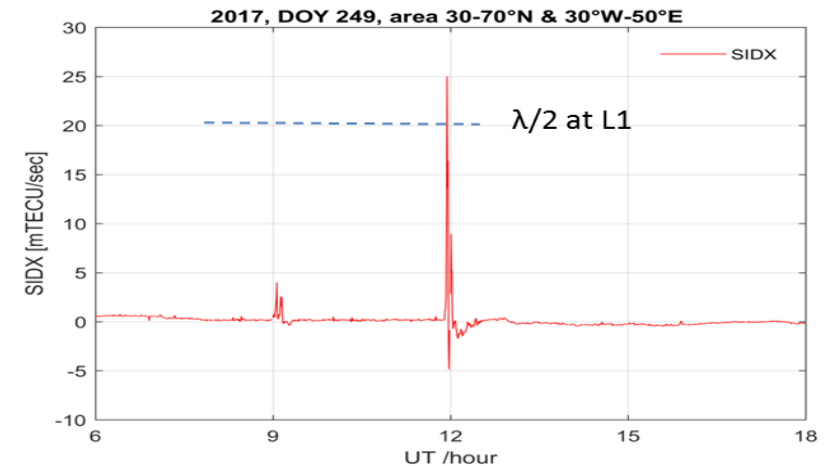
- SIDX – Basic approach:  
Average rate of TEC of all PP  
in a selected area
- SIDX response to solar flares may differ  
from X ray classification due to spectral  
dependence of ionization

$$\frac{\partial TEC}{\partial t} = \frac{\Delta STEC}{M \Delta t} - \frac{\partial TEC}{\partial u} v$$

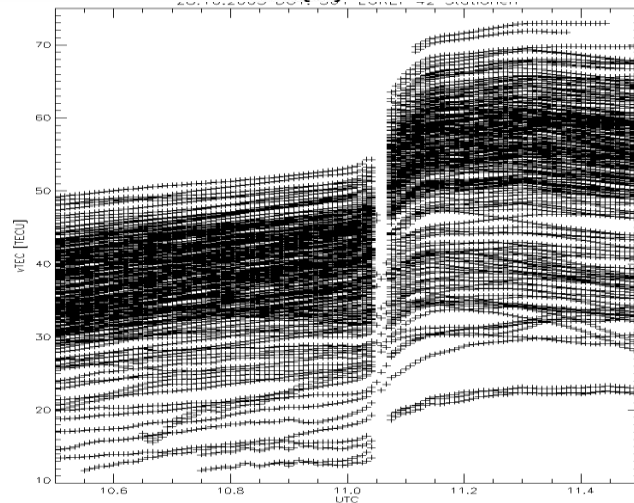
$$\left\langle \frac{\partial TEC}{\partial t} \right\rangle \approx \frac{1}{N} \sum_{i=1}^N \left( \frac{\Delta STEC}{M \Delta t} \right)_i$$

$$SIDX = \left\langle \frac{\partial TEC}{\partial t} \right\rangle$$

$$SIDXS = \sqrt{2 \left( \left\langle \frac{\partial TEC^2}{\partial t} \right\rangle - \left\langle \frac{\partial TEC}{\partial t} \right\rangle^2 \right)}$$



TECr / TECu



Time UT/ hrs.

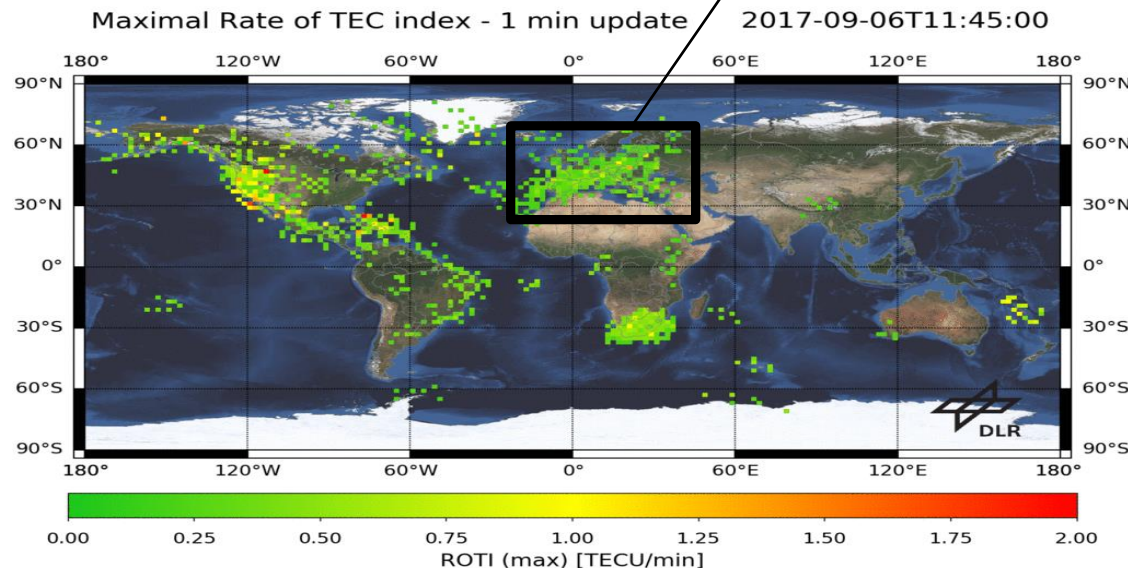
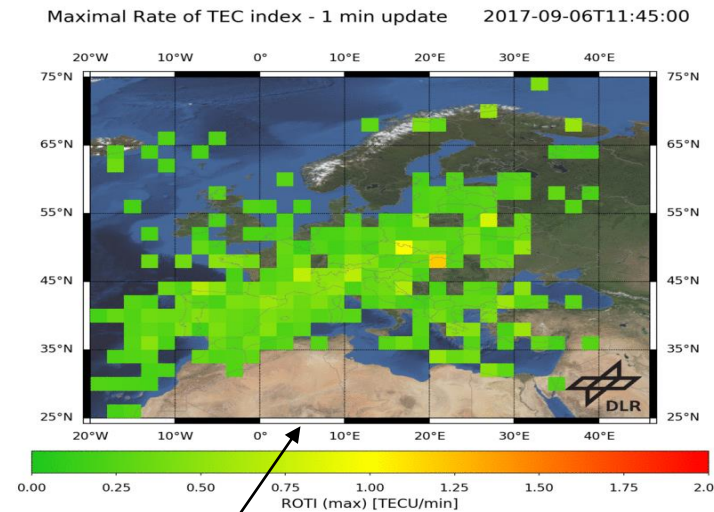


# Space Weather Impact on GNSS – Solar Flare (ROTI)

Solar Flare X9.3  
on September 6, 2017  
at 11:53 UT



Real time ROTI at  
[impc.dlr.de](http://impc.dlr.de)



## Rate Of TEC Index (ROTI)

ROTI and many other indices are currently used to describe ionospheric perturbations for comparative studies e.g. with geomagnetic indices or positioning results.

The NOAA space weather scales G, S, R do not include a scale that addresses explicitly **trans-ionospheric radio wave propagation**.

Considering the broad utilization of space based radio systems like GNSS, an internationally well accepted space weather scale is urgently needed.

The International Space Weather Action Team (ISWAT) initiated by COSPAR addresses many space weather topics.

In **ISWAT G2B-04** we address the topic:  
„Ionospheric perturbation indices and scales“  
(<https://iswat-cospar.org/G2B-04>)

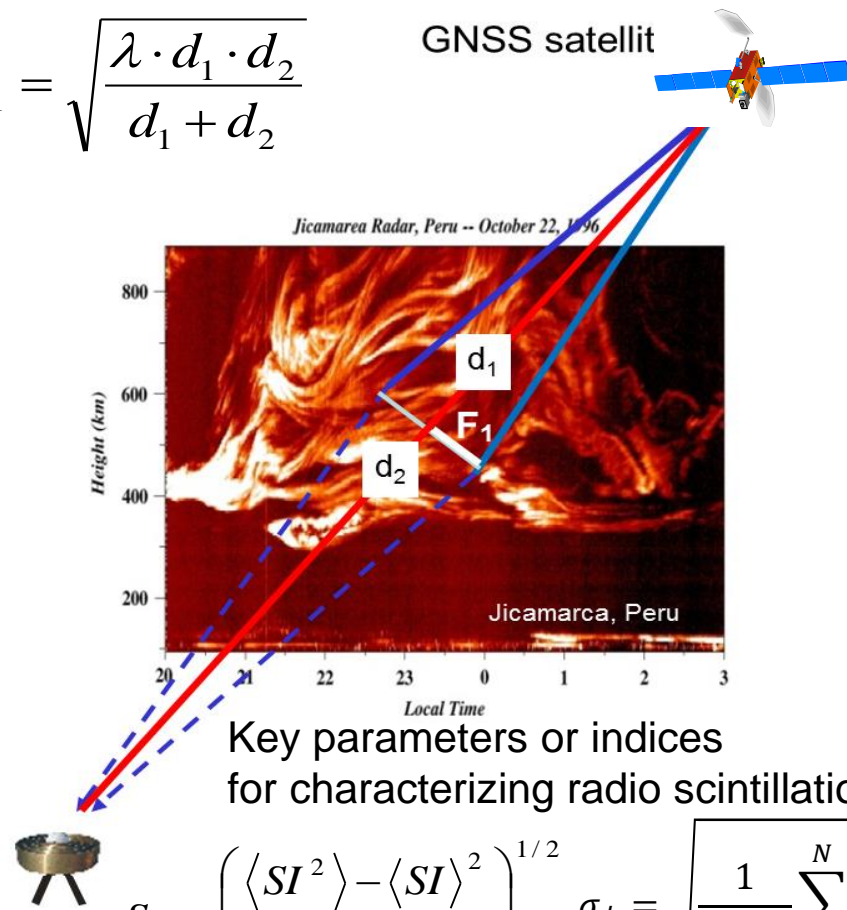
New team members supporting this action are welcome!



# Diffraction effects due to small scale electron density irregularities

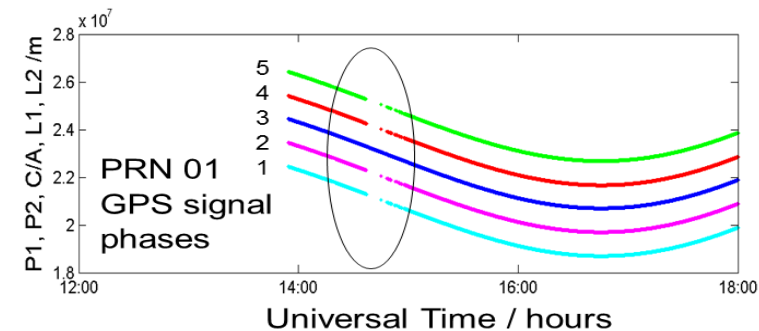
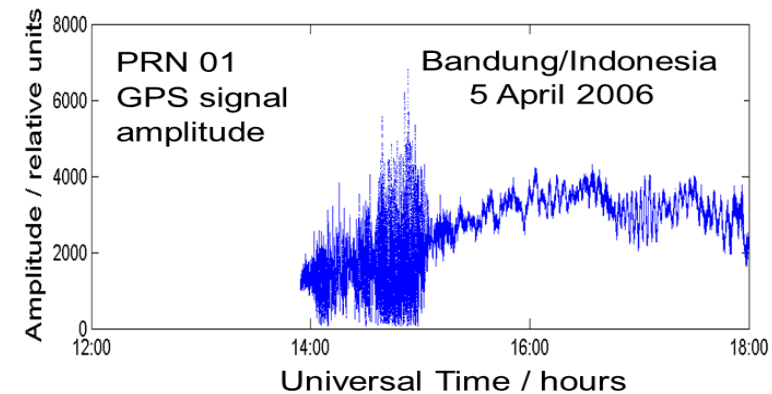
## 1<sup>st</sup> Fresnel zone

$$F_1 = \sqrt{\frac{\lambda \cdot d_1 \cdot d_2}{d_1 + d_2}}$$

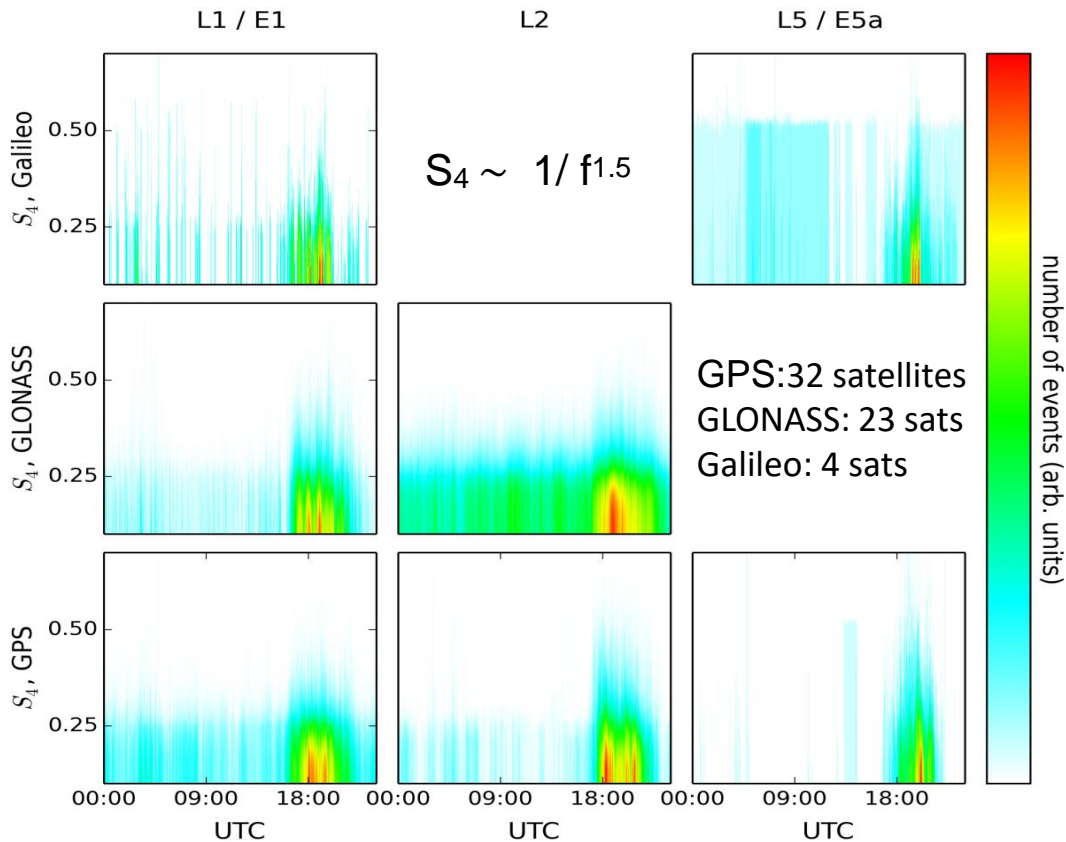


$$S_4 = \left( \frac{\langle SI^2 \rangle - \langle SI \rangle^2}{\langle SI \rangle^2} \right)^{1/2} \quad \sigma_\phi = \sqrt{\frac{1}{N-1} \sum_{i=1}^N (\phi_i - \langle \phi \rangle)^2}$$

- Diffraction and forward scattering of radio waves at small scale ionospheric irregularities may cause strong amplitude and phase fluctuations at ground receivers called: **radio scintillations**

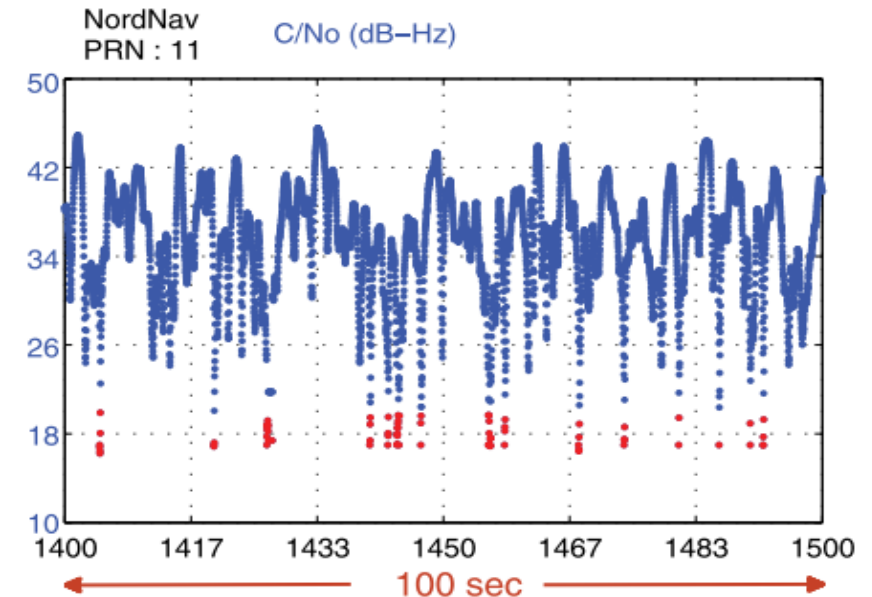


# Impact of radio scintillations on GNSS



All GNSS are affected but in different way.

Hlubek, N. et al. (2014). Scintillations of the GPS, GLONASS, and Galileo signals at equatorial latitude. Journal of Space Weather and Space Climate, 4, A22. <https://doi.org/10.1051/swsc/2014020>



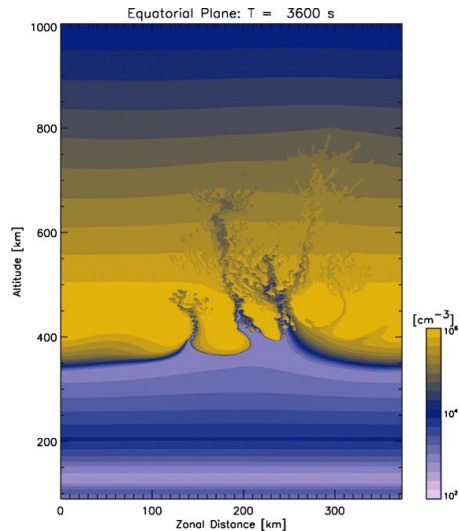
Example of deep signal fades. < 20 dB red

- enhanced noise level
- cycle slips
- loss of lock

Seo, J. et al. (2009), Characteristics of deep GPS signal fading due to ionospheric scintillation for aviation receiver design, Radio Sci., 44, RS0A16, doi:10.1029/2008RS004077.

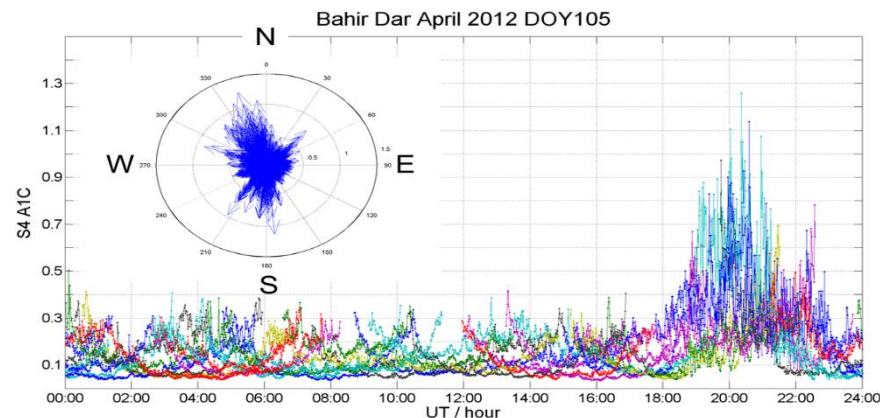


# Scintillation effects – geophysical relationships



## HIRB model

Yokoyama (2017) A review on the numerical simulation of equatorial plasma bubbles toward scintillation evaluation and forecasting, Progress in Earth and Planetary Science (2017) 4:37  
DOI 10.1186/s40645-017-0153-6



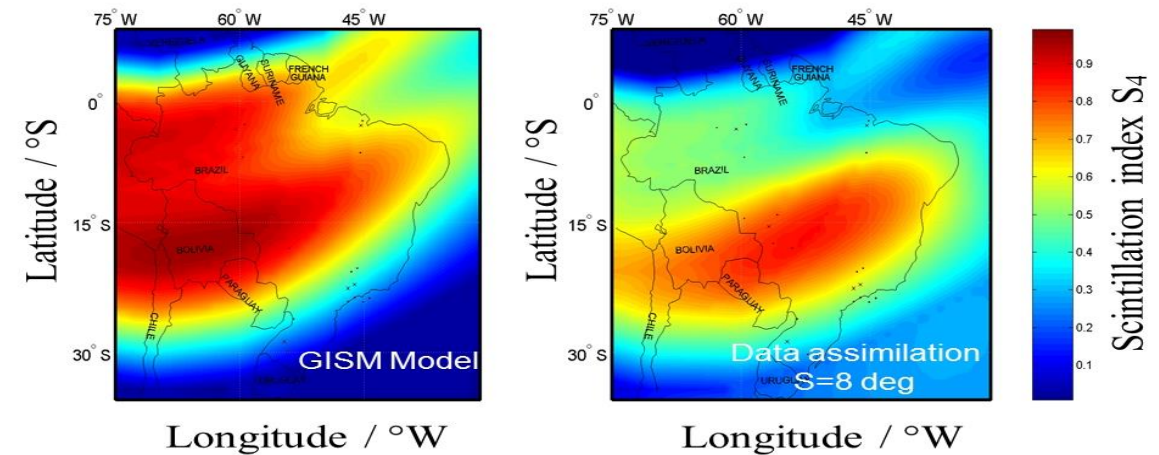
Mersha et al. (2021). On the Relationship between Low Latitude Scintillation Onset and Sunset Terminator over Africa. Remote Sens, 13, 2087. <https://doi.org/10.3390/rs13112087>

Knowledge of physics and occurrence probability as a function of local time and location can help to mitigate scintillation impact on positioning and navigation, e.g. by forecasting.

## Scintillation maps over Brazil on January 11, 2002

Left: GISM model

right: GISM + S4 measurements



Scintillation maps describing the occurrence of scintillation over the user region allow rejecting measurements with ionospheric PPs located in an area with strong scintillation activity. Selection of other satellites with low scintillation activity for positioning.

However: scintillation receivers are costly and rare.

Jakowski, N. (2017) Ionosphere monitoring. In: Springer Handbook of Global Navigation Satellite Systems, Springer Verlag. Seiten 1139-1162. ISBN 978-3-319-429292-7.





# Relationship between ROTI and scintillation index S4

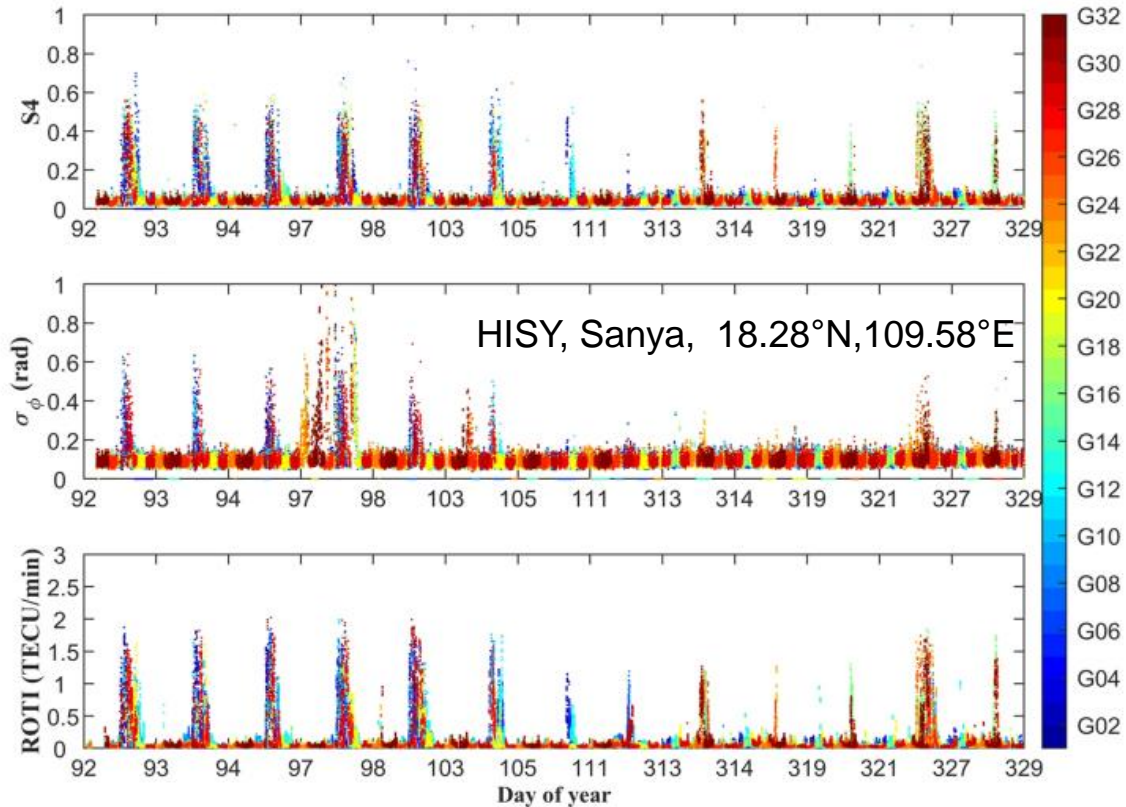


**Figure 1.** Amplitude scintillation index (top), phase scintillation index (middle) and Rate of change of Total electron content Index (bottom) at HISY station in 2015.

Li, W., Song, S., & Jin, X. (2022). Ionospheric scintillation monitoring with ROTI from geodetic receiver: Limitations and performance evaluation. *Radio Science*, 57, e2021RS007420. <https://doi.org/10.1029/2021RS007420>

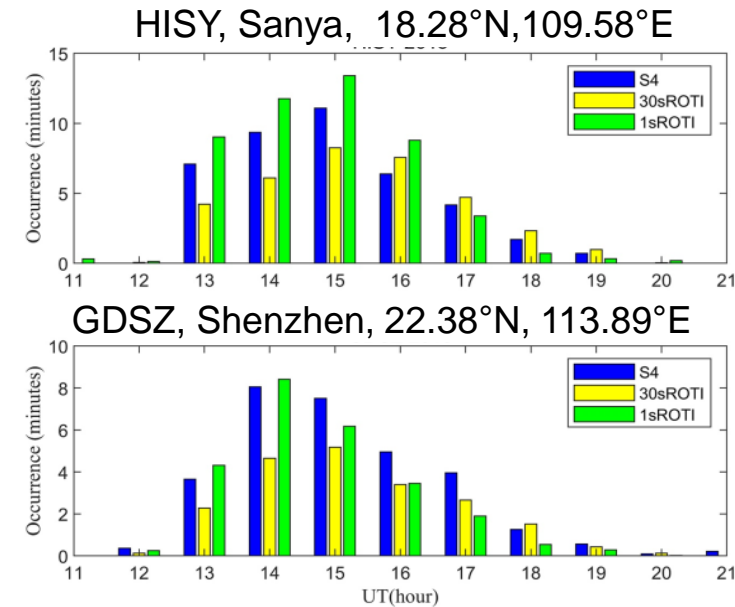


**Figure 3.** Hourly average duration of scintillation monitored by  $S_4$ , 30s-5 min Rate of change of Total electron content Index (ROTI) and 1s-1 min ROTI at HISY (top panel) and GDSZ (bottom panel) in 2015.

There is a close relationship between ROTI and S4

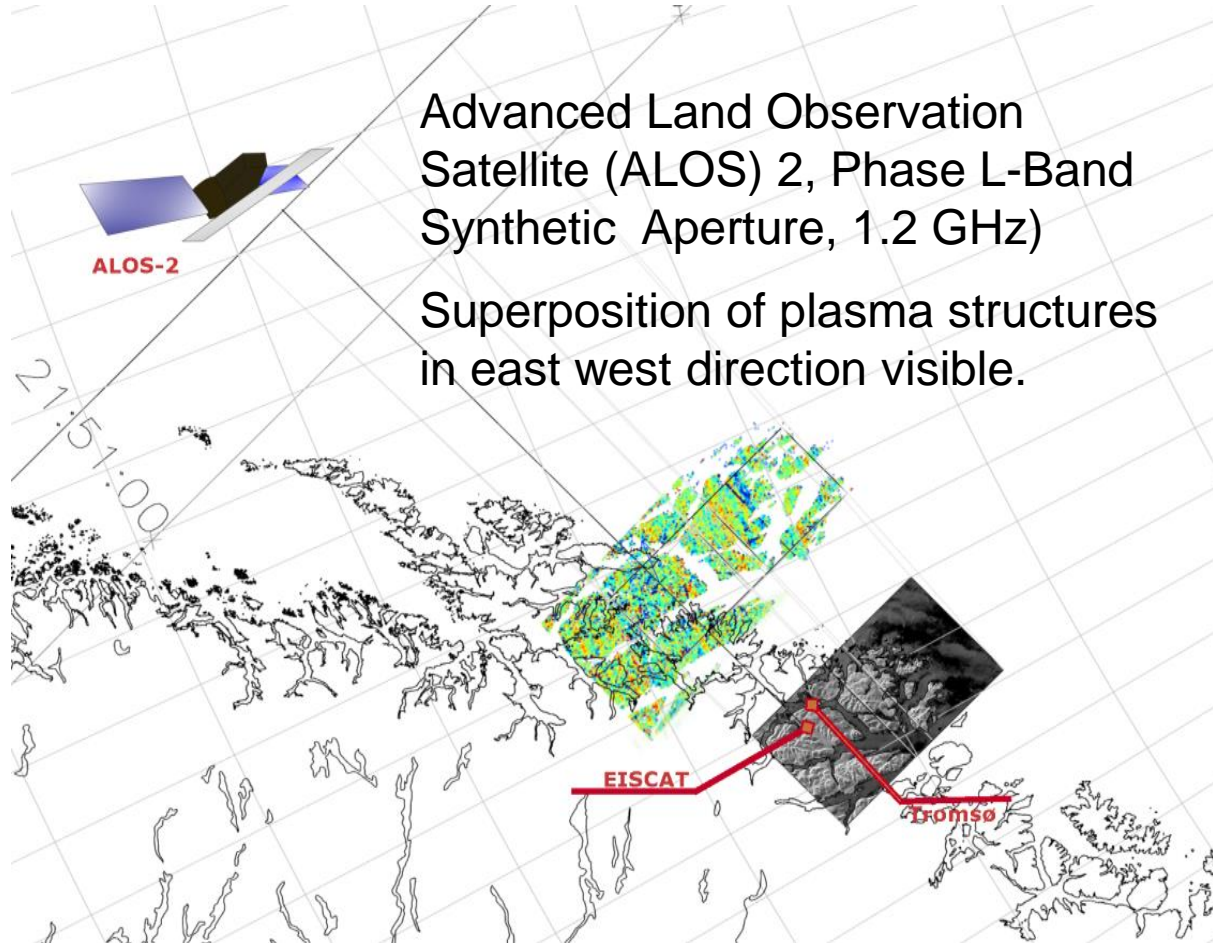
The reliability of ROTI in indicating the occurrence of scintillation can reach 80% and 88% for 30s ROTI and 1s-ROTI, respectively.



**There is a potential for cost-effective monitoring/forecasting of severe radio scintillations causing performance degradation of GNSS and other systems.**



# Space weather impact on remote sensing systems



Advanced Land Observation Satellite (ALOS) 2, Phase L-Band Synthetic Aperture, 1.2 GHz)

Superposition of plasma structures in east west direction visible.

**Remote sensing radar** systems suffer from ionospheric ranging and polarimetric errors.

Remote sensing information is derived from ranging and polarimetric measurements of lineary polarized waves.

Ionosphere impacts

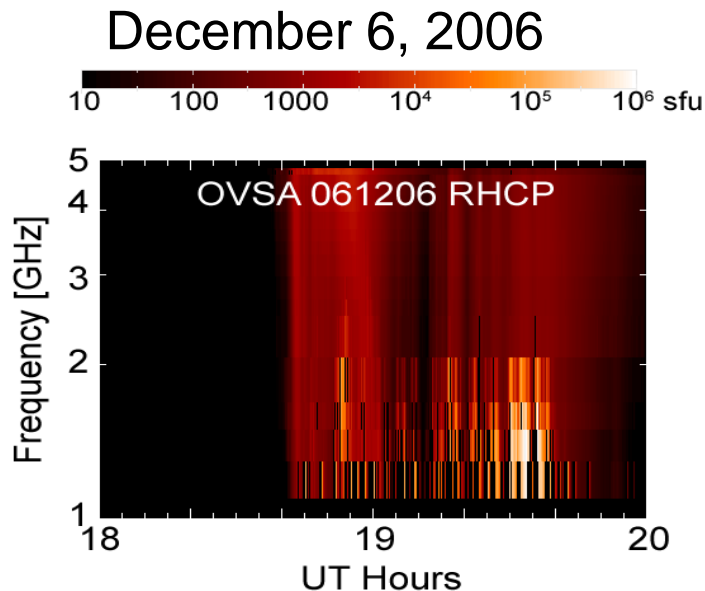
- Ranging: first order effect  $\sim \text{TEC}/f^2$
- Polarimetry: second order effect  $\sim \overline{B \cos \Theta} \cdot \text{TEC} / f^3$

Polarization plane of linearly polarized waves changes with TEC and geomagnetic field

## GNSS Reflectometry

Sato et al., (2018), Imaging high-latitude plasma density irregularities resulting from particle precipitation: spaceborne L-band SAR and EISCAT observations, *Earth, Planets, Space*, 70(1), 163, doi:10.1186/s40623-018-0934-1.

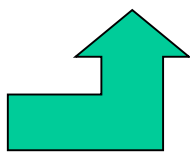
# Interference of solar radio flux with GPS signals



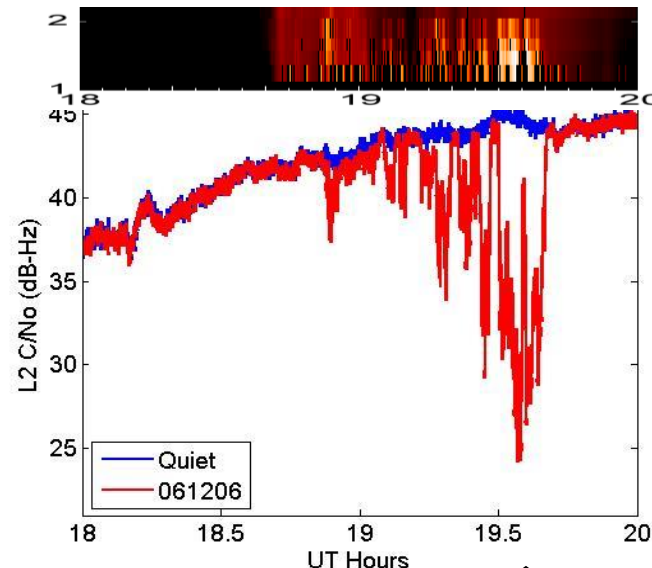
Solar radio burst

up to 150,000 sfu

1 sfu =  $10^{-22} \text{Wm}^{-2}\text{Hz}^{-1}$

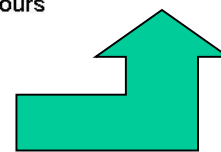


Satcom (UHF) reception is vulnerable against radio bursts in case receiving antennas are in line with the sun.

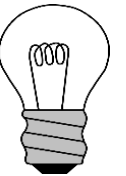


Impact at  
L2- GPS  
signal  
(20 dB loss)

Source: P. Doherty

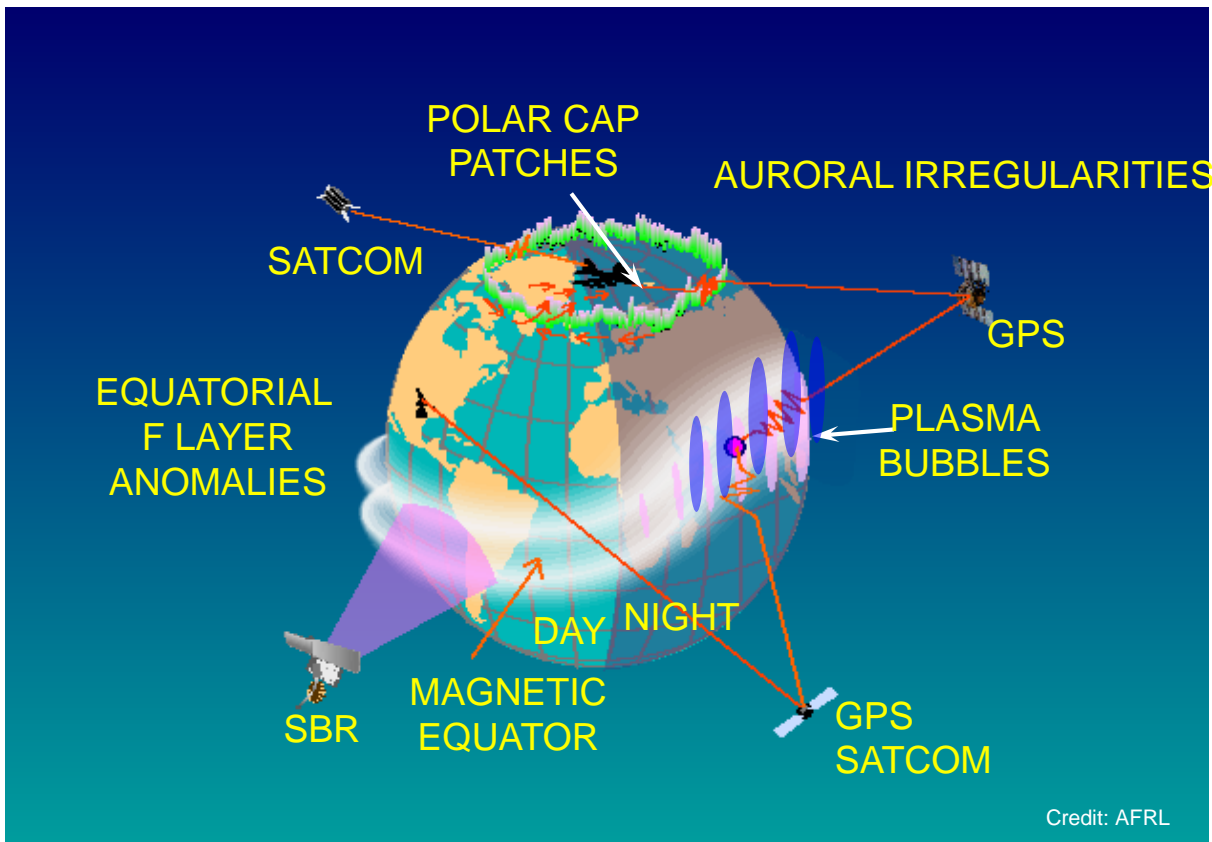


- Intense Solar Radio Bursts (SRBs) at L-band are a source of Radio Frequency Interferences (RFI) for Global Navigation Satellite Systems (GNSS) and space based communication in UHF (Satcom).
- GPS/GLONASS transmitted power is about 20-300 Watt.
- Considering the orbit altitude of 20200 km the received signal is very weak.
- Air traffic control centres in Stockholm and Malmö, Sweden noticed that radar stations of the Swedish Air Navigation Service Provider were not relying on November 4, 2015.
- Solar radio burst interference index dedicated to GNSS single and double frequency users supports GNSS.
- GNSS signals may heavily be disturbed also by man made radio noise in the L-band (Jamming).

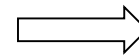




# Summary



- Radio signals used in HF communication, space based navigation and radar systems are impacted by the ionospheric plasma due to refraction, absorption, diffraction and scattering.
- Ionospheric delay is the largest error source for single-frequency GNSS and a significant factor for DGNSS.
- Ionospheric storms and small scale irregularities may cause performance degradation in precise / SoL GNSS applications and remote sensing systems.
- Monitoring, modeling and forecasting of ionospheric behavior and derived n.r.t. products like proper indices will further support mitigating ionospheric impact on radio signals as used in telecommunication, space based navigation and remote sensing.

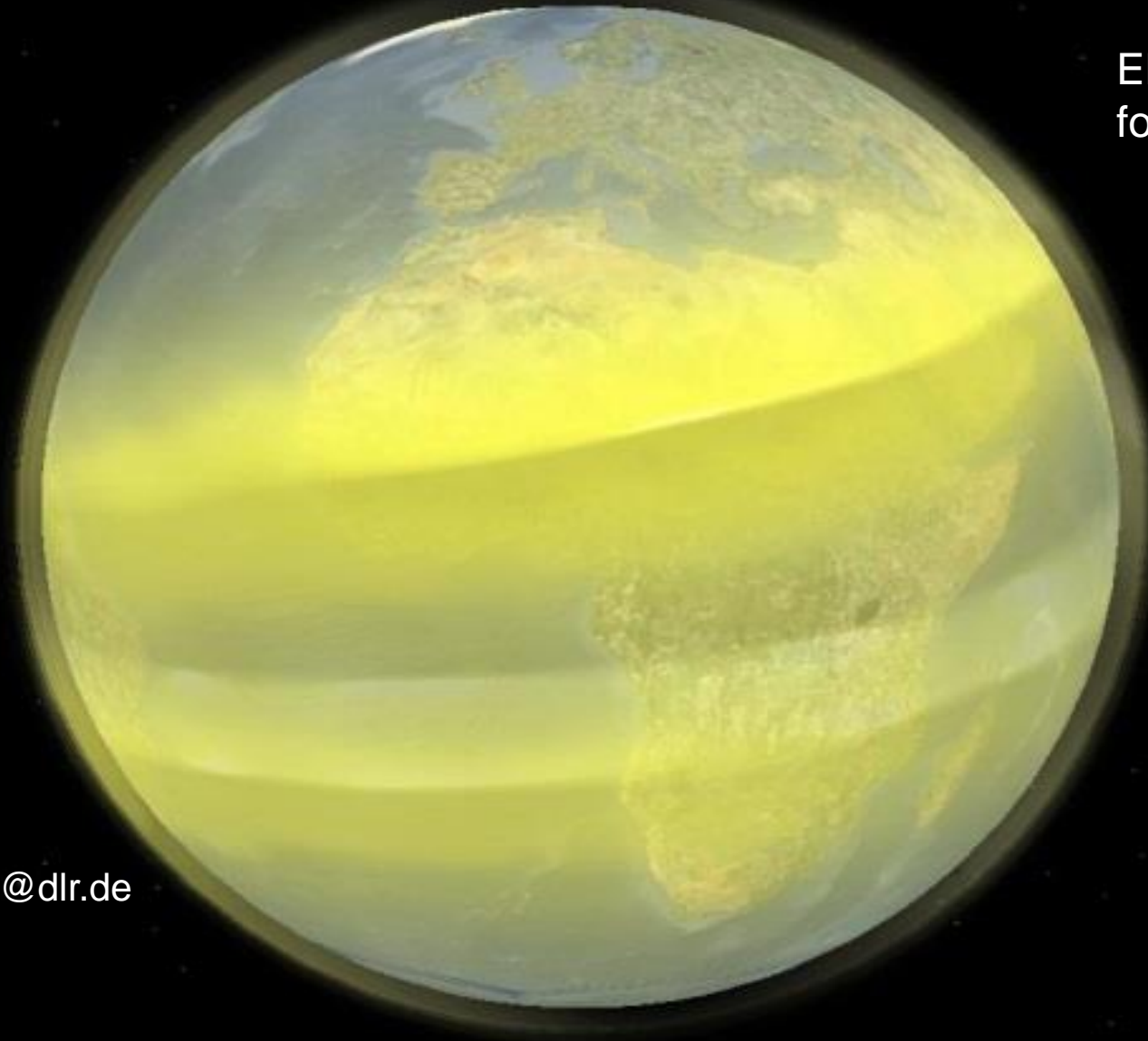


Challenge of future work



# Ionosphere from space

Electron density reconstruction  
for July 23, 2011, 14:00 UT



**Thank you  
for your  
attention!**

Contact:  
Dr. Norbert Jakowski  
Kalkhorstweg 53  
D-17235 Neustrelitz  
Germany  
Email: [Norbert.Jakowski@dlr.de](mailto:Norbert.Jakowski@dlr.de)  
Web: <http://impc.dlr.de>



Data SIO, NOAA, U.S. Navy, NGA, GEBCO  
Image IBCAO  
© 2011 Cnes/Spot Image

©2010 Google